ORNL/Sub/97-SY009/1

Oxide Dispersion Strengthened Fe₃Al-Based Alloy Tubes: Application Specific Development for the Power Generation Industry

Report Prepared by

Bimal K. Kad
University of California-San Diego, La Jolla, CA 92093-0085

Under
19X-SY009C

for
OAK RIDGE NATIONAL LABORATORY
Oak Ridge, Tennessee 37831

Managed by
UT-Batelle LLC

for the
DEPARTMENT OF ENERGY
Under contract DE-AC05-96OR22464

July 2001

Oxide Dispersion Strengthened Fe$_3$Al-Based Alloy Tubes:
Application Specific Development for the Power Generation Industry

Table of Contents

Oxide Dispersion Strengthened Fe₃Al-Based Alloy Tubes: Application Specific Development for the Power Generation Industry

Summary

A detailed and comprehensive research and development methodology is being prescribed to produce Oxide Dispersion Strengthened (ODS)-Fe_3Al thin walled tubes, using powder extrusion methodologies, for eventual use at operating temperatures of up to 1100°C in the power generation industry. A particular 'in service application' anomaly of Fe_3Al-based alloys is that the environmental resistance is maintained up to 1200°C, well beyond where such alloys retain sufficient mechanical strength. Grain boundary creep processes at such high temperatures are anticipated to be the dominant failure mechanism.

Thus, the challenges of this program are manifold: 1) to produce thin walled ODS-Fe_3Al tubes, employing powder extrusion methodologies, with 2) adequate increased strength for service at operating temperatures, and 3) to mitigate creep failures by enhancing the as-processed grain size in ODS-Fe_3Al tubes.

Our research progress till date has resulted in the successful batch production of typically 8 Ft. lengths of 1-3/8" diameter, 1/8" wall thickness, ODS-Fe_3Al tubes *via* a proprietary single step extrusion consolidation process. The process parameters for such consolidation methodologies have been prescribed and evaluated as being routinely reproducible. Such processing parameters (*i.e.*, extrusion ratios, temperature, can design etc.) were particularly guided by the need to effect post-extrusion recrystallization and grain growth at a sufficiently low temperature, while still meeting the creep requirement at service temperatures. Static recrystallization studies show that elongated grains (with their long axis parallel to the extrusion axis), typically 200-2000μm in diameter, and several millimeters long can be obtained routinely, at 1200°C. The growth kinetics are affected by the interstitial impurity content in the powder batches. For example complete recrystallization, across the tube wall thickness, is observed for clean powders (PMWY-3) and consequently this powder batch exhibits the best creep performance. Prolonged exposures (about 700 hours) at 10Ksi at 1000°C have been achieved till date. The high impurity content powder batches (PMWY-1 and PMWY-2) exhibit modest improvements in tensile and creep response behavior at 1000°C upon further selective heat-treatments intended to increase grain size.

Introduction

Fe$_3$Al-based alloys are promising materials for high temperature, high pressure, tubing applications, due to their superior corrosion resistance in oxidizing, oxidizing/ sulphidizing, sulphidizing, and oxidizing/chlorinating environments. Such high temperature corroding environments are nominally present in the coal or gas fired boilers and turbines in use in the power generation industry. Currently, hot or warm working of as-cast ingots by rolling, forging or extrusion in the 650-1150°C temperature range is being pursued to produce rod, wire, sheet and tube products [1,2]. *A particular 'in service application' anomaly of Fe$_3$Al-based alloys is that the environmental resistance is maintained up to 1200°C, well beyond where such alloys retain sufficient mechanical strength.* Thus, powder metallurgy routes, incorporating oxide dispersions (ODS), are required to provide adequate strength at the higher service temperatures.

The target applications for ODS-Fe$_3$Al base alloys, in the power generation industry, are thin walled (0.1" thick) tubes, about 1 to 3 inches in diameter, intended to sustain internal pressures (P) of up to 1000psi at service temperatures of 1000-1200°C. The economic incentive is the low cost of Fe$_3$Al-based alloys and its superior sulphidization resistance, in comparison to the competing Fe-Cr-Al base alloys and the Ni-base superalloys currently in service.

Program Particulars

In December 1997, the University of California-San Diego (UCSD) was awarded a research subcontract to engage in a detailed and comprehensive research and development effort to produce thin walled ODS-Fe$_3$Al tubes, using powder extrusion methodologies, for eventual use at operating temperatures of up to 1100°C in the power generation industry. Grain boundary dominated creep processes at such high service temperatures are anticipated to be the dominant failure mechanism.

Within the framework of this intended target application, the development of suitable materials containing Y$_2$O$_3$ oxide dispersoids, must strive to deliver both a combination of high mechanical strength at temperature, as well as prolonged creep-life in service. Such design requirements are often at odds with each other, as strengthening measures severely limit the as-processed grain size, detrimental to creep life. Thus post-deformation recrystallization, or zone annealing, processes are necessary to increase the grain size, and possibly modify the grain shape for the anticipated use.

In this current project we address manufacturing issues and development efforts towards our stated development goal. The challenges of this program are many-fold: 1) to produce thin walled ODS-Fe$_3$Al tubes, employing powder extrusion methodologies, with 2) adequate increased strength for service at operating temperatures, and 3) to mitigate creep failures by enhancing the as-processed grain size in ODS-Fe$_3$Al tubes. The detailed task structure is shown in Figure 1. The project is iterative in nature, intended to systematically examine the various sub-processes for optimum performance and cost considerations. This entails i) prescription of material compositions and consolidation methodologies (single vs. multiple step) to create tubes, ii) prescribing zone annealing and recrystallization schedules to create large grain sized creep resistant tubes, and iii) direct verification of improved high temperature response.
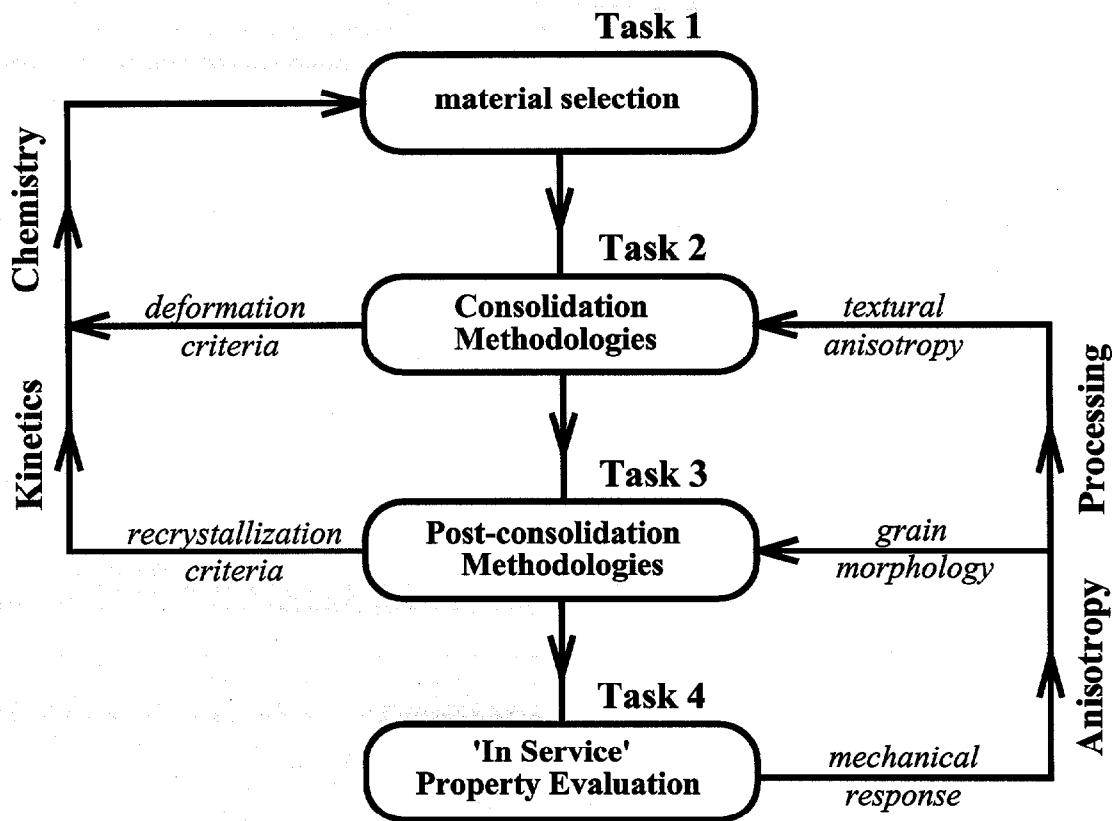
2

Task 1

```
        material selection
```

Task 2

```
    deformation    Consolidation    textural
    criteria       Methodologies    anisotropy
```

Task 3

```
  recrystallization  Post-consolidation   grain
    criteria         Methodologies        morphology
```

Task 4

```
                   'In Service'       mechanical
                Property Evaluation   response
```

Chemistry **Kinetics** **Processing** **Anisotropy**

Figure 1. Schematic of the iterative research and development methodology for ODS-Fe₃Al based alloy tubes.

Progress Status and Report

This report describes the processing, microstructure and properties of ODS-Fe₃Al alloy tubes, with a view to improving the high temperature creep response. Our work has focused on all **Tasks 1-4** illustrated in Figure 1, and our progress in these tasked areas is outlined below, in iterative sequence. The progress reported here has been previously described in Quarterly Management Reports, and in the 12th. 13th, 14th and 15th Fossil Energy Conference Reports [6,7].

Our research has resulted in the successful batch production of typically 8 Ft. lengths of 1-3/8" diameter, 1/8" thick ODS-Fe₃Al tubes *via* a proprietary single step extrusion consolidation process. The process parameters for such consolidation methodologies have been prescribed and evaluated as being routinely reproducible. Such processing parameters (*i.e.*, extrusion ratios, temperature, can design etc.) are particularly guided by the need to effect post-extrusion recrystallization and grain growth at a sufficiently low temperature, while still meeting the creep requirement at service temperatures. Static recrystallization studies show that elongated grains (with their long axis parallel to the extrusion axis), typically 200-2000µm in diameter, and several millimeters long can be obtained routinely in selected compositions, at 1200°C. However, such grain growth does not necessarily span the entire wall thickness. The recrystallized region is most commonly bounded by unrecrystallized rings at the outer an inner periphery of the tube thickness, their relative dimensions dictated by the specific level of impurity. The ensuing creep response varies with the overall grain structure.

Progress: Iteration 1

The Fe_3Al + 0.5% Y_2O_3 composition mix was tentatively optimized at ORNL, and three separate batches were milled, identified as PMWY-1, PMWY-2 PMWY-3 in Table 1, details of which are available elsewhere [3]. PMWY-1 powder batch contained the maximum amount of interstitial impurities, and PMWY-3 the minimum. For the purposes of initial extrusion consolidation, the intermediate level impurity powder PMWY-2 was employed.

Experimental efforts were undertaken to consolidate the ODS powder, to produce sound stock material to be used for materials characterization and preliminary recrystallization studies. In this first iteration powder consolidation extrusions were carried out in carbon steel cans.

Table 1: Chemical analyses of the as-received and milled powder batches

Element	As-Received HM	As-Received PM	PMWY-1	PMWY-2	PMWY-3
Fe	Bal.	79.6			
Al	16.3	18.20			
Cr	2.4	2.18			
Zr	20 ppm	26 ppm			
O (total)	60 ppm	110 ppm	1800 *ppm*	1900 *ppm*	1400 ppm
O (in Y_2O_3)			1025 *ppm*	1053 *ppm*	1080 ppm
O balance			775 *ppm*	847 *ppm*	320 ppm
O *pickup*			**665 *ppm***	**737 *ppm***	**210 ppm**
N	18 ppm	7 ppm	1264 *ppm*	145 *ppm*	88 *ppm*
N *pickup*			**1257 *ppm***	**138 *ppm***	**81 *ppm***
C		24 ppm	667 *ppm*	360 *ppm*	303 *ppm*
C *pickup*			**643 *ppm***	**336 *ppm***	**279 *ppm***
H		16 ppm	115 *ppm*	40 *ppm*	29 *ppm*
C+N+O *pickup*			**2565 *ppm***	**1211 *ppm***	**570 *ppm***

(Bulk compositions are identified in wt%)

The carbon steel cans were 51-mm OD x 6.4 mm wall x 125 mm length (2-in x 0.25-in x 5-in). The cans were filled with powder, evacuated and sealed. A total of three cans were prepared for direct consolidation of powder into solid bars, the details of which are provided in Table 2.

Table 2: Extrusion consolidation parameters for PMWY-2 powders

Extrusion Number	Temperature	Die Size mm	Die Size inch	Area Reduction	Tonnage
5016[a]	900	16.3	0.64	9.8:1	266
5014[a]	1000	12.7	0.50	16.0:1	290
5013[a]	1100	12.7	0.50	16.0:1	180
5030[b]	1000	25.4	1.00	12.25:1	532

[a]51mm (2.0 in) billets for solid extrusion; [b]82mm (3.5 in) billet for tube extrusion.

As-extruded Mechanical Anisotropy

Knoop hardness measurements were made on longitudinal sections of extruded rods, in directions parallel (0° degrees), inclined (45° degrees) and perpendicular (90° degrees) to the elongated grains. Figure 2 shows the hardness response of the three extrusions, where the data scatter represents variations along the radial dimension of the extrusions. Both the 0° and 90° hardness measurements follow the expected decline with increasing extrusion temperature. The 45° indents show anomalous behavior with temperature. Nonetheless, the strength anisotropy was relatively small (about 5%), and the material was deemed mechanically isotropic.
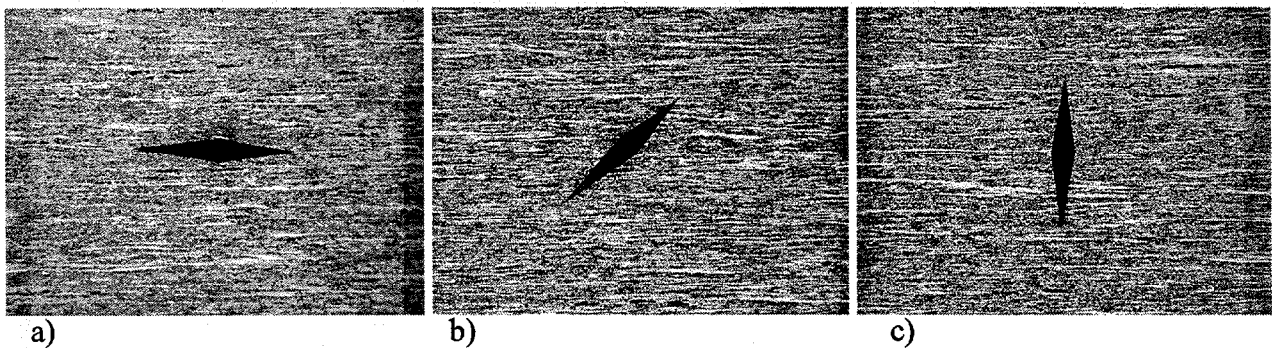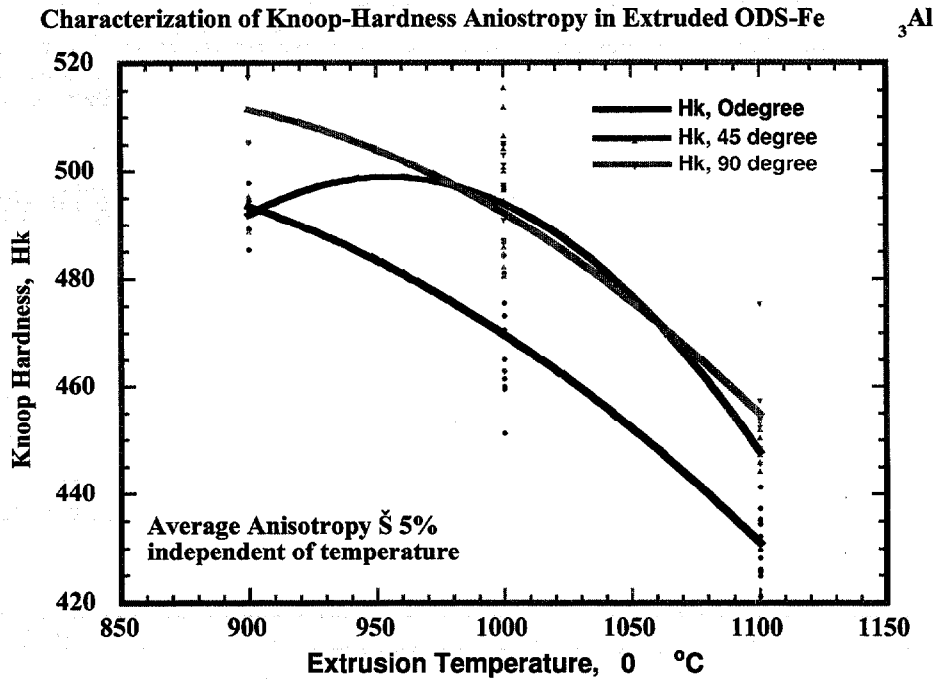
Characterization of Knoop-Hardness Aniostropy in Extruded ODS-Fe$_3$Al

a)   b)   c)

Figure 2. Knoop-hardness characterizations of the as-extruded ODS-Fe$_3$Al rods in the a) parallel (0°), b) inclined (45°), and c) perpendicular (90°) orientations.

As-extruded Texture Anisotropy

The ODS-Fe$_3$Al powder extrusions exhibited an extreme texture anisotropy, as observed earlier for cast and extruded Fe$_3$Al base alloys [5]. A strong {011}<uvw> fiber texture was observed along the extrusion axis, as recorded via X-ray diffraction peaks from transverse and

longitudinal sections. A direct comparison of the {022} diffraction peaks taken as a general measure of stored energy, Figure 3, indicated diminishing line broadening with extrusion temperature. Several observations are apparent from such measurements: 1) the extrusions show an extreme anisotropy of {011} diffraction intensity in the longitudinal and transverse directions for each of the extrusions, and 2) the relative anisotropy increases with extrusion temperature, and 3) the {011}<uvw> fiber texture is progressively stronger with extrusion temperature.
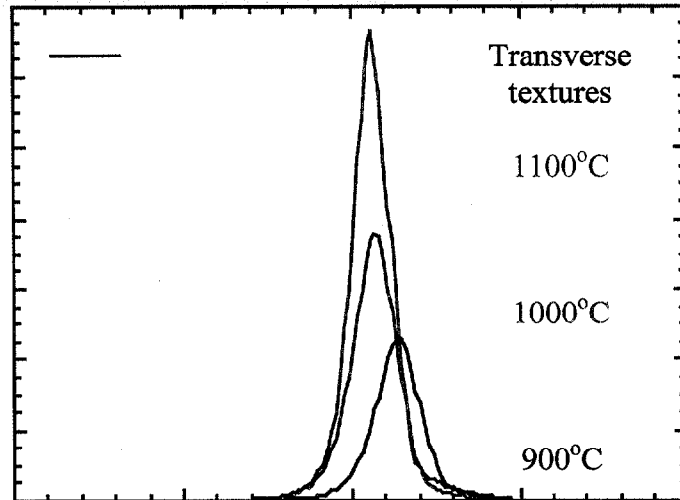

Figure 3. Comparison of {022) textural alignment with increasing extrusion temperature.

Recrystallization Kinetics

In this first iteration, recrystallization kinetics was studied only for the 900°C extrusion, of a lower extrusion ratio of 9.8:1. Samples were spark machined from the rod cross-section and heat-treated in air using a muffle furnace at 1100-1300°C for 1 hour. Figure 4 shows the respective optical micrographs of longitudinal sections of as-extruded, and the heat-treated specimen. Figure 5 shows the hardness response of the heat-treated samples where the as-extruded hardness of 530 DPH falls to about 340 DPH for the specimen treated at 1300°C. A large drop in strength occurred at 1100°C in the recovery stage, where no appreciable grain growth was observed. We also noted that a small hardness plateau was observed in the 1200-1250°C temperature range, beyond which the hardness continued to decrease, along with the observation of exaggerated grain growth. While complete recrystallization was obtained at 1300°C, this was accompanied by increased void formation in the solid rods. Thus, the processing parameters required a revision, in the following iteration, to enhance the kinetics, and reduce the recrystallization temperature.
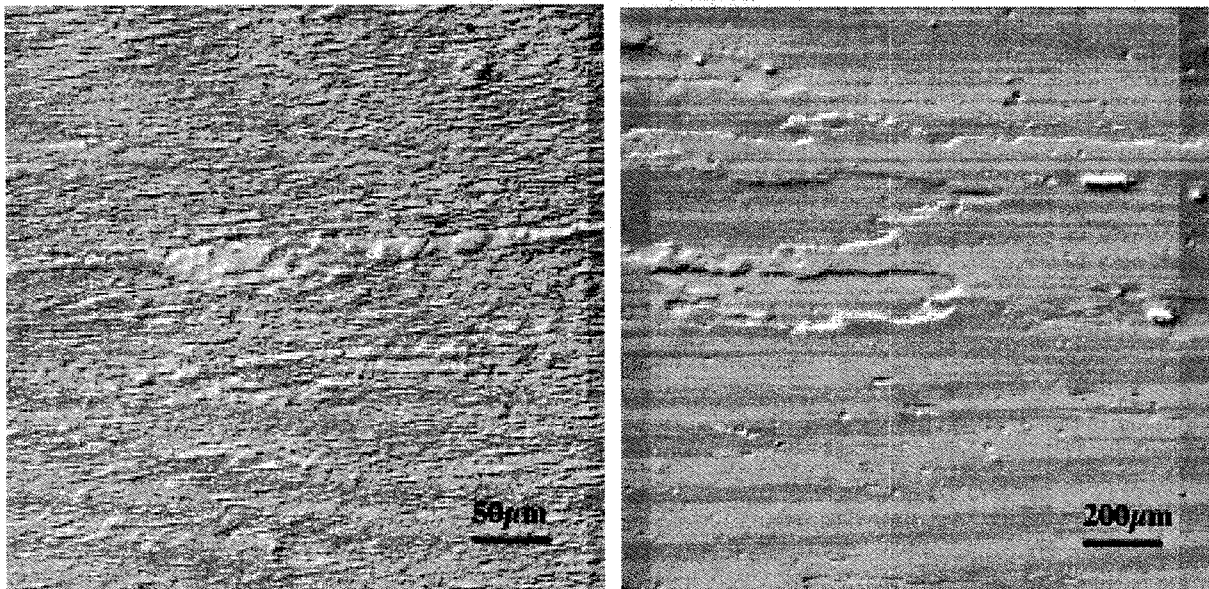
Figure 4. Optical micrographs of a) as-extruded rod, and b) heat-treated at 1300°C/1hr.
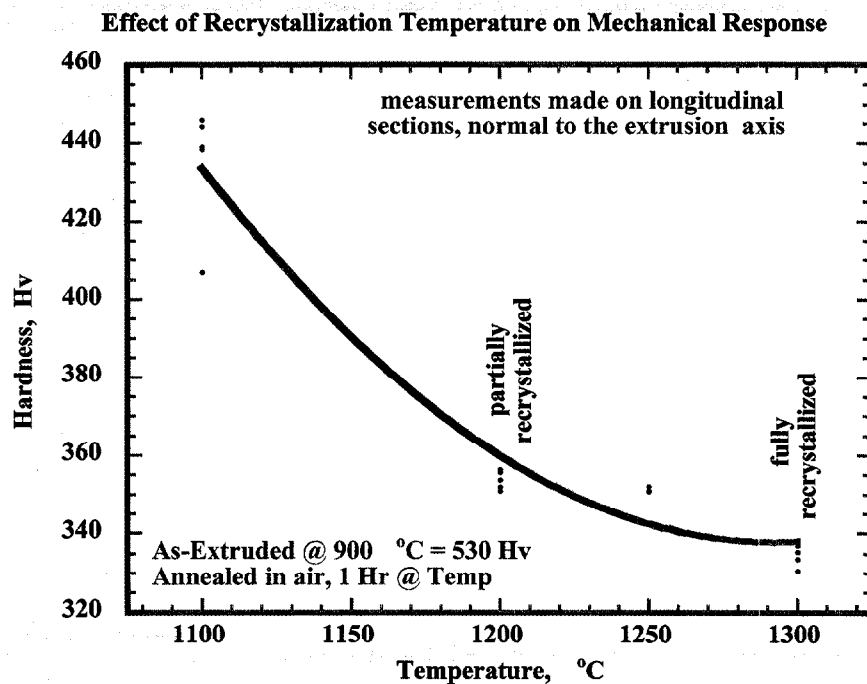

Effect of Recrystallization Temperature on Mechanical Response

Figure 5. Vickers Hardness decay in response to the recrystallization heat-treatments.

Recrystallization Kinetics with Pre-Strain

A set of specimens was deformed in compression ($e \approx 8\%$, 16%), along the prior extrusion axis, at strain rates of $\approx 10^{-3}$ sec^{-1}. The specimens exhibited cracking along the compression axis, but were nonetheless heat-treated at 1100°C and 1200°C for one hour. Figure 6 shows hardness response due to the various thermal treatments. A small amount of prestrain was particularly helpful at the lower temperatures of 1100°C in promoting grain growth, but this effect was essentially non-existent for treatments at 1200°C. Figure 7 shows a direct comparison of the

longitudinal section microstructures of the as-extruded, as heat-treated, and pre-strained + heat-treated samples, where the latter exhibited a grain size of the order of 25μm. It was deemed likely that such pre-straining, or increasing the extrusion deformation strain, may be employed to accelerate the recrystallization kinetics, as attempted in iteration 2.
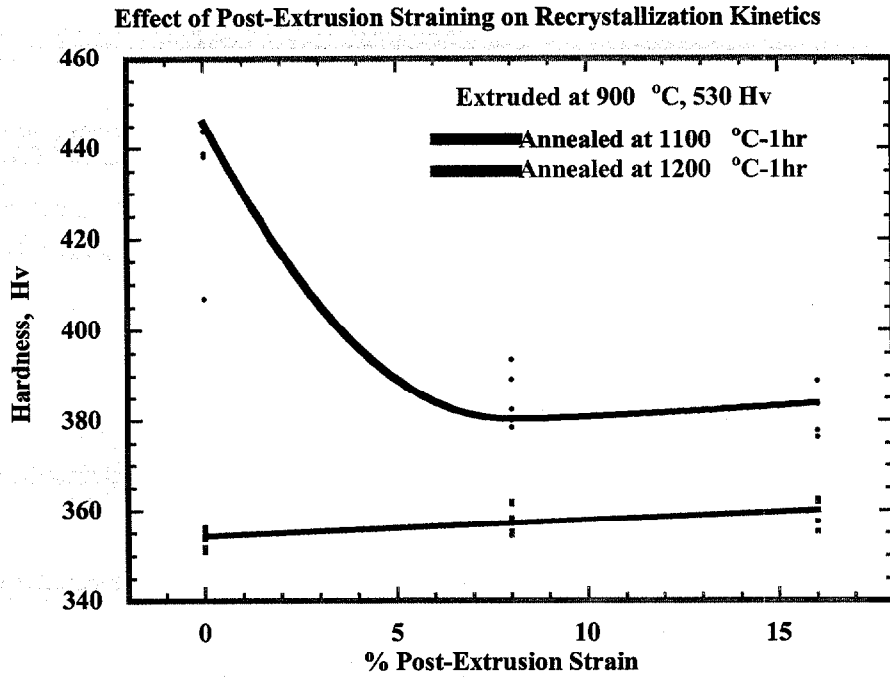

Figure 6. Hardness response of recrystallized specimens with and without pre-straining.
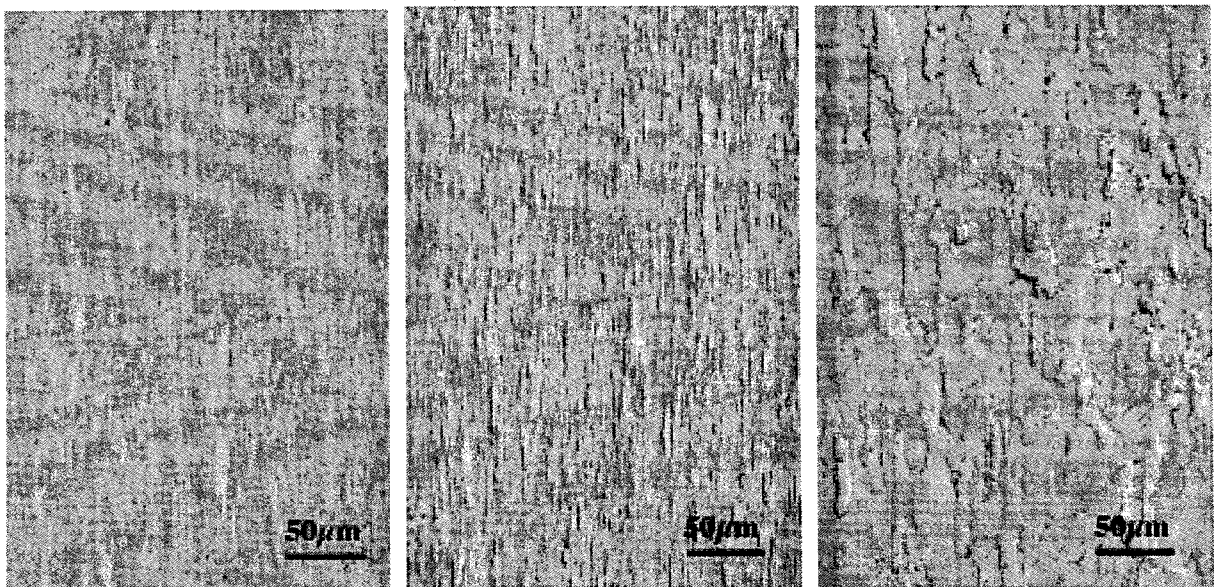

Figure 7. Comparison of a) as-extruded, b) heat treated at 1100°C-1hr, and c) pre-strained and heat-treated at 1100°C-1hr.

Progress: Iteration 2

At the conclusion of the first iteration, the broad parameters of extrusion consolidation were identified. Furthermore, it was shown that the recrystallization kinetics of an as-extruded stock material could be altered via post-extrusion straining techniques, as illustrated in Figures 6-7. However post-extrusion straining bears a certain cost, and thus a revised extrusion schedule was attempted on a second batch of extrusions to incorporate greater deformation strain.

In this second iteration, powder consolidation extrusions of PMWY-1, PMWY-2 and PMWY-3 material batches were carried out in carbon steel billets. Each of the carbon steel cans measured 51-mm OD x 6.4 mm wall x 125 mm length (2-in x 0.25-in x 5-in). The cans were filled with powder, evacuated and sealed. A total of three cans were prepared for direct consolidation at a 16:1 extrusion ratio, at 1000°C, the details of which are provided in Table 3.

Table 3: Extrusion consolidation parameters for PMWY-1-3 powders

| Extrusion | | Die Size | | Area | |
Material	Temperature	mm	inch	Reduction	Tonnage
PMWY-1[a]	1000	12.7	0.50	16.0:1	≈310
PMWY-2[a]	1000	12.7	0.50	16.0:1	≈290
PMWY-3[a]	1000	12.7	0.50	16.0:1	≈290

[a]51mm (2.0 in) billets for solid rod extrusion;

As-extruded Texture Anisotropy

A strong {011}<uvw> fiber texture was observed along the extrusion axis for each of the extruded rods of PMWY-1, PMWY-2, and PMWY-3 materials. A direct comparison of the {022} diffraction peaks for the transverse and longitudinal sections of the extruded rods is shown in Figure 8a-b. Results indicated that the textural alignment was the strongest for PMWY-1 and the weakest for PMWY-2. A further examination of the transverse versus longitudinal textures in each of the rods indicated that PMWY-1 exhibited the maximum anisotropy of ≈25 whereas this anisotropy was only of the order of 8-10 for the PMWY-2 extrusion. This variation in anisotropy is not well understood, particularly as the extrusion parameters were essentially identical for all the three bars. Nonetheless, these parameters are routinely tracked in an effort to establish correlations with recrystallization kinetics and characteristics.

Recrystallization Kinetics

A marked improvement in recrystallization kinetics was observed with this increased extrusion ratio. All the rods exhibit partial to complete recrystallization (grain size ≈ 1-2 mm) with the heat treatment schedule not exceeding 10 hours at 1200°C. For brevity, the grain growth behavior of PMWY-1 and PMWY-2 rods is shown in Figures 9 and 10, respectively. In the cross- section view of Figure 9, the outer region is recrystallized, while the core (about 50%) is
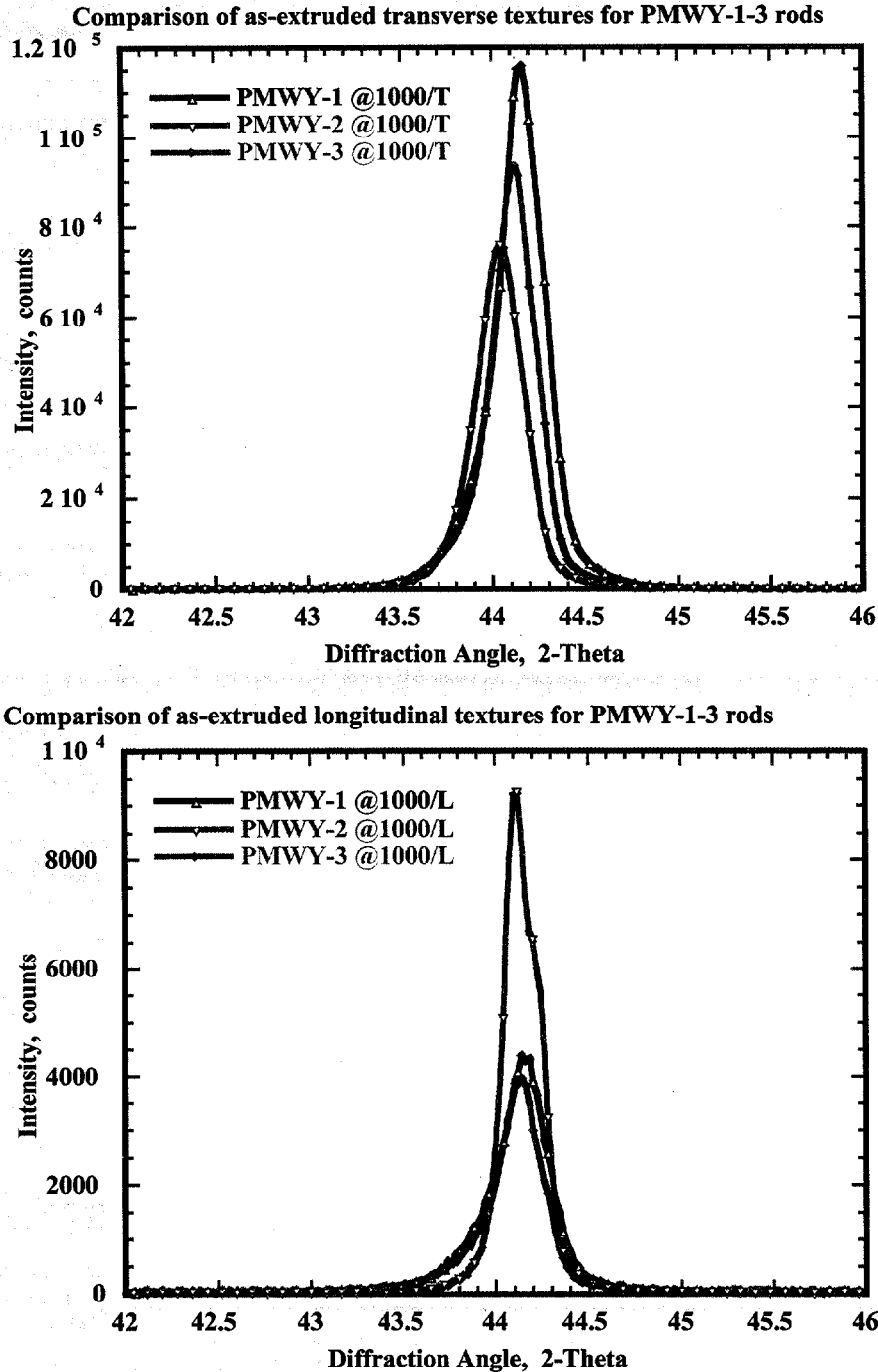
Comparison of as-extruded transverse textures for PMWY-1-3 rods

Comparison of as-extruded longitudinal textures for PMWY-1-3 rods

Figure 8.   Comparison of {022} texture alignment in the a) transverse and b) longitudinal sections of PMWY-1, PMWY-2 and PMWY-3 extruded rods.

essentially un-recrystallized. However, for the PMWY-2 material, Figure 10, the exterior is essentially a single grain, and the central section is comprised of multiple grains, with grain size of the order of 1-2 mm. Furthermore, the grain shape morphology is extremely contorted, with inter-penetrating segments.
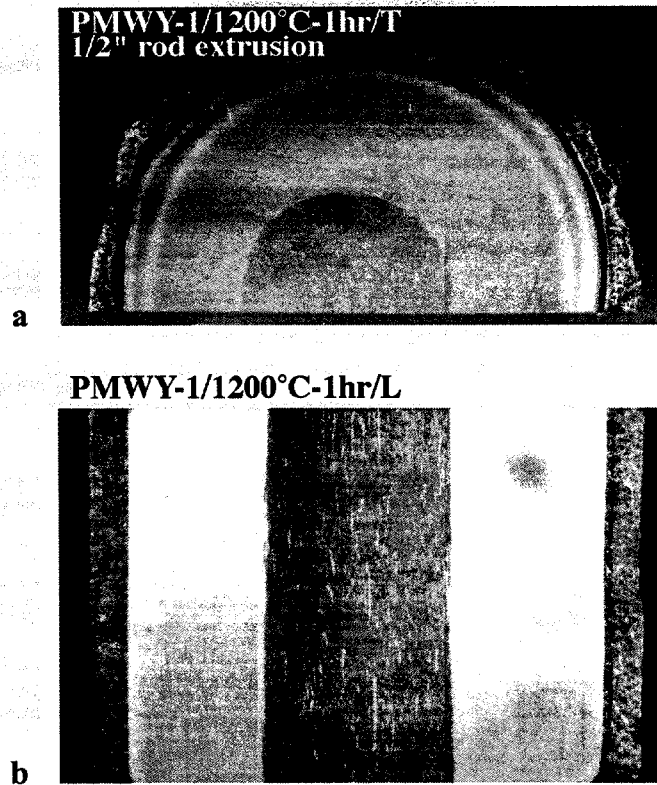
Figure 9. Optical micrographs of a) transverse, and b) longitudinal sections of the 1/2"
extruded rod of PMWY-1 material, heat-treated at 1200°C-1hr.

Figure 10. Optical micrographs of transverse section of the 1/2" extruded rod of PMWY-
2 material, heat-treated at 1200°C-1hr.

The interpenetrating nature of the grains is further illustrated in Figure 11, as extracted from
transverse sections of the PMWY-2 sample. The grains essentially exhibit a cactus like structure
with the net result of providing mechanical interlocking between adjacent grains. The etching
contrast in the cross-section view of Figure 10a, indicates several such interpenetrating islands.
Such features are considered important from the viewpoint of developing creep-resistant
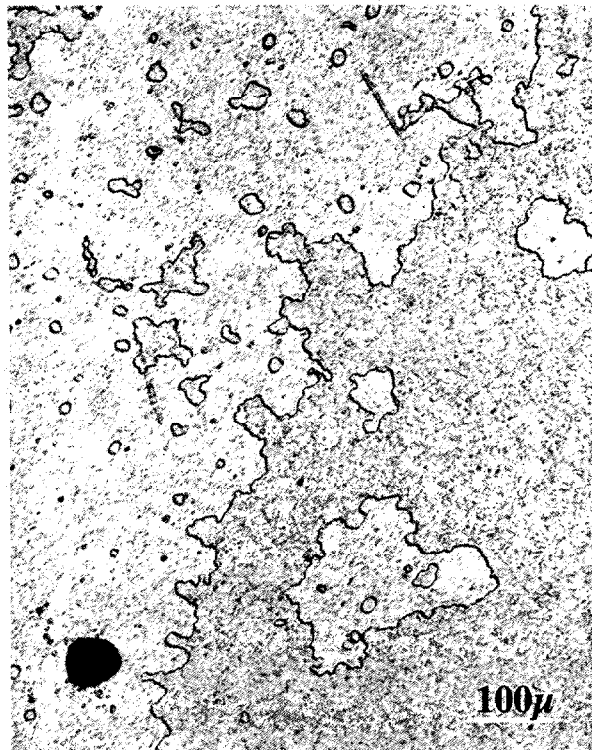materials, and will be particularly examined in Task 4 of this program.

Figure 11. Optical micrograph of the interpenetrating recrystallized/unrecrystallized grain structure in the transverse sections of the extruded PMWY-2 rods. (heat-treatments conducted in the 1100°-1200°C range). The outer section (left) is recrystallized while inner section remains un-recrystallized.

Progress: Iteration 3

Following the second iterative process, it was concluded that the modified extrusion parameters continued to yield sound extruded stock, with a marked increase in recrystallization kinetics. Thus large grain size grain sized material was obtained by routine heat-treatments in the 1100-1200° range, with hold times of less than 100 hours.

In this third iteration, the process parameters developed and refined in iterations 1 and 2 for rod stock, were applied to annular extrusions in an effort to directly produce tube stock. We note here that annular extrusions were a modification prescribed and accepted during the course of this research program. Typically tube products are produced *via* a two stage process, *i.e.*, the first step involves creating a bulk ingot of a cylindrical cross-section, which is then re-worked to a hollow tube using different production methodologies. For specialty alloys and materials, this process typically involves drilling a center hole (*i.e.*, gun drilling) before sizing the tube to required dimensions. In our modified process, it was proposed to combine the consolidation step with the tube drilling step *via* the use of an annular extrusion can. The relative manufacturing advantages and disadvantages of this single step process are illustrated briefly in Figure 12.

The benefits of this single step process are readily apparent, and four different extrusions were attempted as described in Table 4. Thus about 6-8 Ft. lengths of 1-3/8" diameter, 1/8" wall thickness, ODS-Fe$_3$Al tubes were produced *via* the single step extrusion consolidation process.

12

Comparsion of Tube Extrusion Methodologies

multiple step	single step
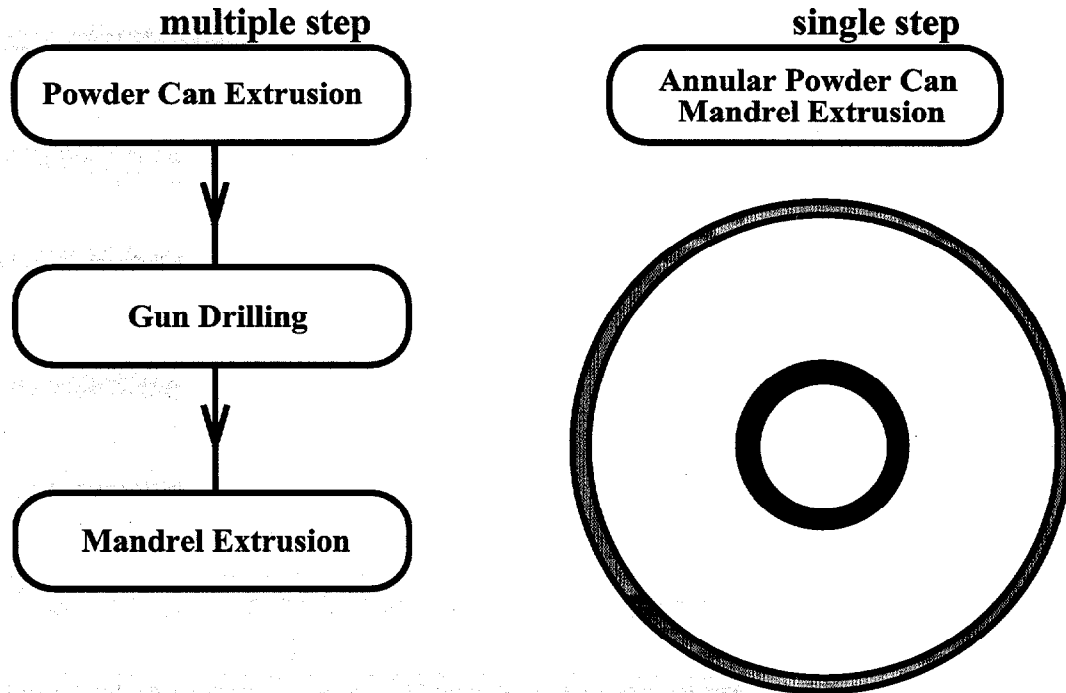
Advantages:

Clean inner surface

Better dimensional tolerance

Disadvantages:

multiple heating/extrusion steps

poor product yield

Advantages:

energy efficient manufacturing

improved product yield

Disadvantages

annular can design complexities

inside surface can layer removal

Figure 12: Comparison of single vs. multiple step extrusion consolidation methodologies.

Table 4: Tube extrusion consolidation parameters for PMWY-1-3 powders

Extrusion		Die Size	Mandrel Size	Area	Area
Material	Temperature	inch	inch	Reduction	Tonnage
PMWY-1[a]	1000°C	≈1.375	1.00	≈16.0:1	NA
PMWY-2[a]	1000°C	≈1.375	1.00	≈16.0:1	NA
PMWY-2[a]	1000°C	≈1.375	1.00	≈16.0:1	NA
PMWY-3[a]	1000°C	≈1.375	1.00	≈16.0:1	NA

Figure 13 shows a set of tubes in the as-extruded as well as in the surface finished condition. The surface finishing is intended to remove only the outside steel case, and no attempt was made to remove the inside steel case. The tubes were of sound quality, and exhibited no cracking and/or damage after routine machining operations.

Figure 13. Assorted ODS-Fe$_3$Al tubes in the as-extruded (below), and surface finished (top) condition, as produced from an annular can (top left) consolidation methodology.

Hardness Properties & Recrystallization Kinetics

The micro-hardness measurements on longitudinal sections of the as-extruded, and the recrystallized tubes, are illustrated in Figure 14. The as-extruded hardnesses were of the order of 450-480 DPH, with PMWY-1 material being the hardest and PMWY-3 the softest. In previous iterations, it was ascertained that large recrystallized grains could be produced by heat-treatments in the 1100°C-100hrs to 1200°C-10 hours range. Thus, in this iteration, the heat-treatment schedules were focused to three sets of conditions as; i) 1100°C for 100 hrs, ii) 1200°C for 1-hr, and iii) 1200°C for 10 hrs.

The heat-treated tubes yielded nearly flat (i.e., stable) hardness profile for the three heat-treatment schedules, Figure 14, with the exception of PMWY-2 tubes heat-treated at 1200°C-1hr exhibiting some softening at the extended hold time. This flat profile was concomitant with a recrystallized state, similar to that observed previously for 1/2" rod extrusions (see Figure 5, *iteration 1*). For example PMWY-1 had the highest level of interstitial impurities and PMWY-3 the least, which correlated with PMWY-1 exhibiting a higher micro-hardness in the as-extruded

and the heat-treated conditions. This correlation with interstitial impurity (introduced during the milling process) points to a possible avenue of additional strength improvements.

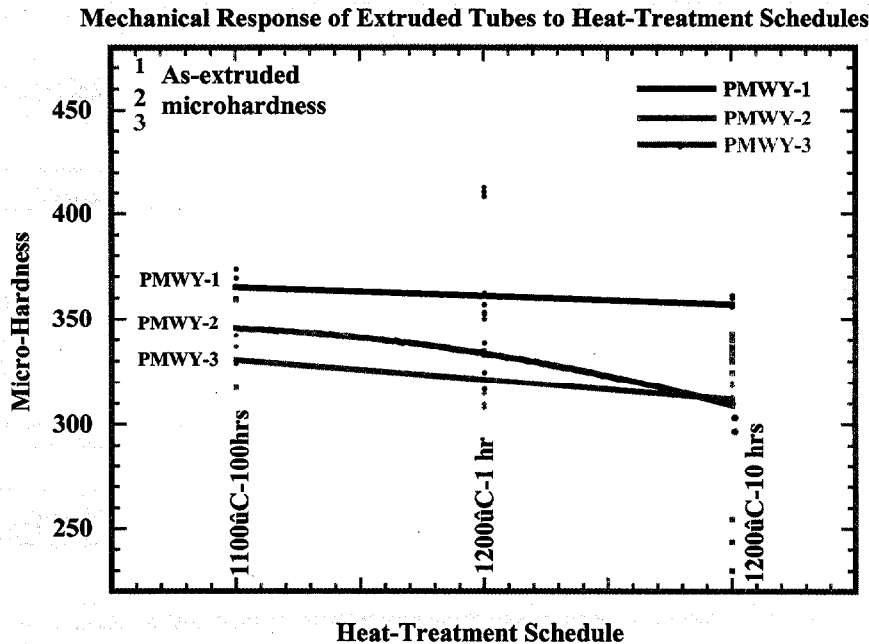**Mechanical Response of Extruded Tubes to Heat-Treatment Schedules**

Figure 14. Material microhardness response in the as-extruded, as well as recrystallized state, for the PMWY-1, PMWY-2 and PMWY-3 extruded tubes. Note that the near flat hardness profile indicates a stable microstructural state for all the powder batches.

Recrystallized Grain Shapes & Morphologies

For the sake of brevity, we report here a single set of longitudinal and transverse micrographs for the PMWY-1, PMWY-2 and PMWY-3 tubes heat-treated at 1200°C for 1 hr. A generic view of the entire cross-section of the sectioned tubes is shown in Figure 15, indicating large-scale grain growth along the tube circumference.

Figure 16a-b shows the longitudinal and transverse views of the PMWY-1 tube respectively, over the entire wall-thickness, including the exterior (at left) and interior (at right) steel-case. A reaction zone about 200μm thick was observed on the exterior surface of the Fe_3Al tube, and was characterized by grain boundaries aligned roughly along the radial direction. In the Fe_3Al tube, three distinct regions are observed over the wall thickness, as illustrated *via* etching contrast differences in the longitudinal and cross-section views. Note that only the middle region of the tube thickness is recrystallized. The roughly 700μm wide recrystallized zone is bounded by unrecrystallized regions about 500μm and 2000μm wide on the exterior and interior surfaces of the tube respectively. Thus while recrystallization is initiated within the wall thickness (about 25% of wall thickness), at this temperature, it does not extend to the extremities. Most importantly, these regions are extended along the circumfurential direction, akin to rings fitting over each-other. This grain alignment is particularly noteworthy, for pressurized tubes, where the tangential loading is twice as severe as the longitudinal loading.
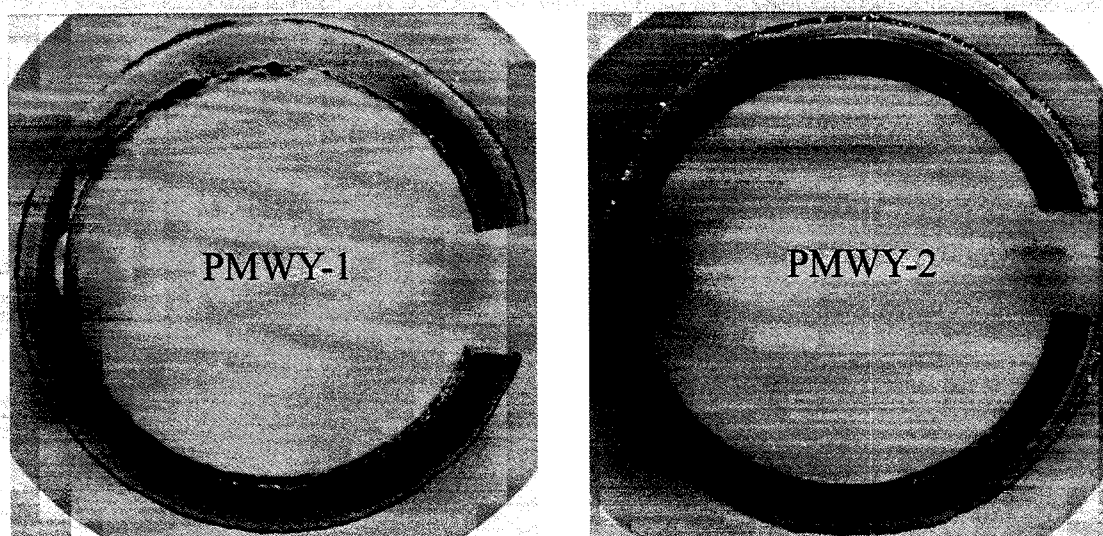
15

Figure 15. Cross-sectional macro views of the heat-treated a) PMWY-1, and 2) PMWY-2 tubes. Note three distinct regions circumfurentially aligned across the tube wall span.

Figure 17a-b shows the longitudinal and transverse views of the PMWY-2 tube, over the entire wall-thickness, including the exterior (at left) and interior (at right) steel-case. A reaction zone about 225µm thick was observed on the exterior surface of the Fe3Al tube. Once again three regions are observed – a recrystallized region about 2000µm wide is bounded by about 500µm and 700µm wide strips of unrecrystallized regions on the outside and the inside surface respectively. The recrystallized region spans roughly 60% of the tube wall thickness. Both the exterior and interior extremities of the Fe3Al tube were characterized by the familiar tangentially oriented un-recrystallized regions extending over the entire circumference of the tube. Interestingly the recrystallized region is populated by an assortment of inter-penetrating grains expected to be beneficial to creep response.

Figure 18a-b shows the longitudinal and transverse views of the PMWY-3 tube, over the entire wall-thickness, including the exterior (at left) and interior (at right) steel-case. A reaction zone about 225µm thick is observed on the exterior surface of the Fe3Al tube. Unlike PMWY-1 and PMWY-2 tubes, there were no regions of circumferentially aligned grains. But the entire section thickness is fully recrystallized. Though large jagged and interpenetrating grains were observed throughout the transverse and longitudinal sections, often spanning the entire wall thickness, they did not extend circumferentially. The existence of these inter-penetrating features is expected to beneficially impact creep response. Additionally, PMWY-3 tubes heat-treated at 1100°C-100hrs and 1200°C-10hrs (not shown here) also exhibited similar grain morphologies.

The kinetics of grain growth are consistent with the overall interstitial impurity content of the respective powder batches. While recrystallization is initiated in all tube sections for this constant heat-treatment, the increased impurity precipitate content hinders its growth. Thus PMWY-3 with the least impurity exhibits large-scale grain growth while PMWY-2 and PMWY-1 show limited grain growth on account of their increasing impurity content (see Table 1).
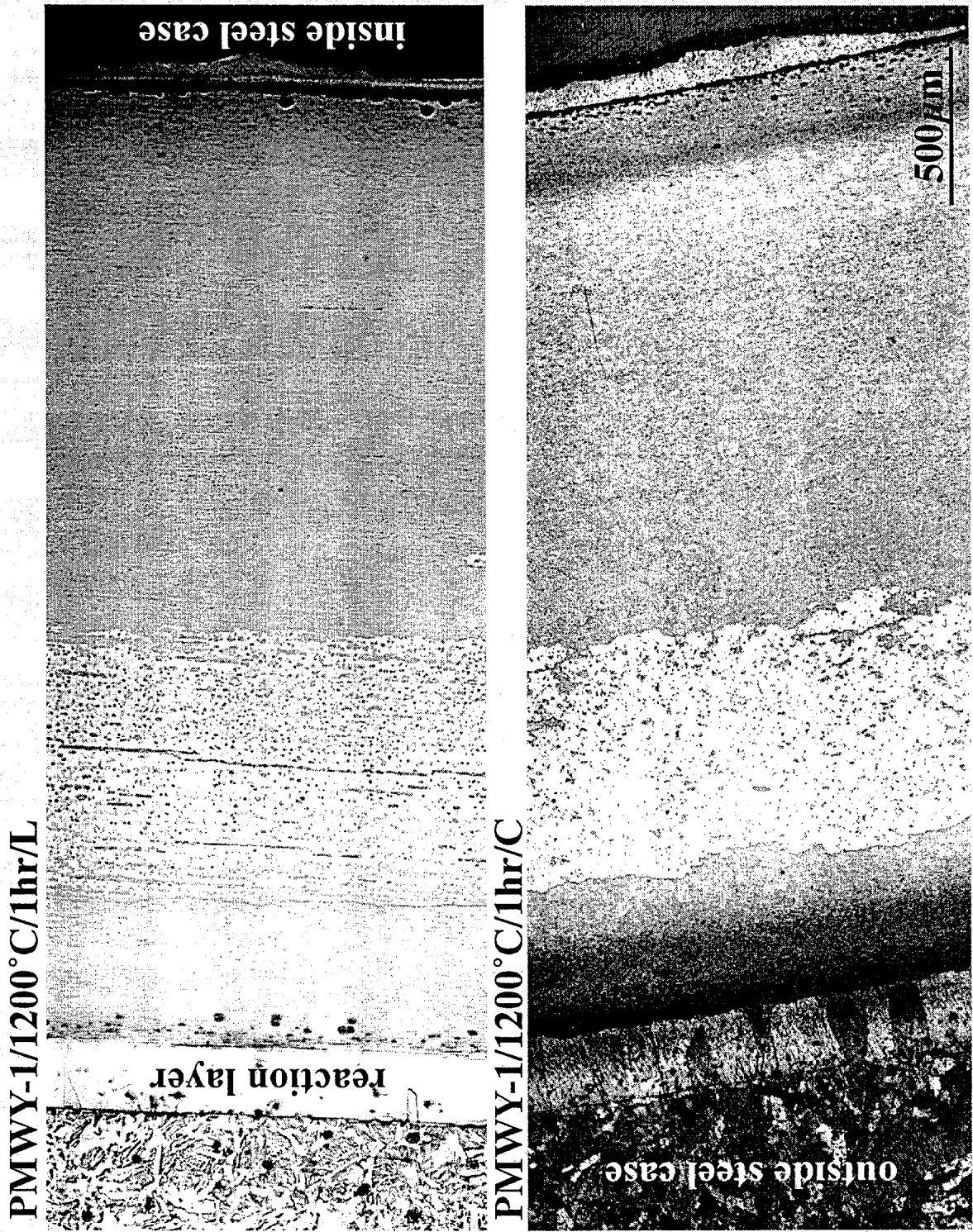
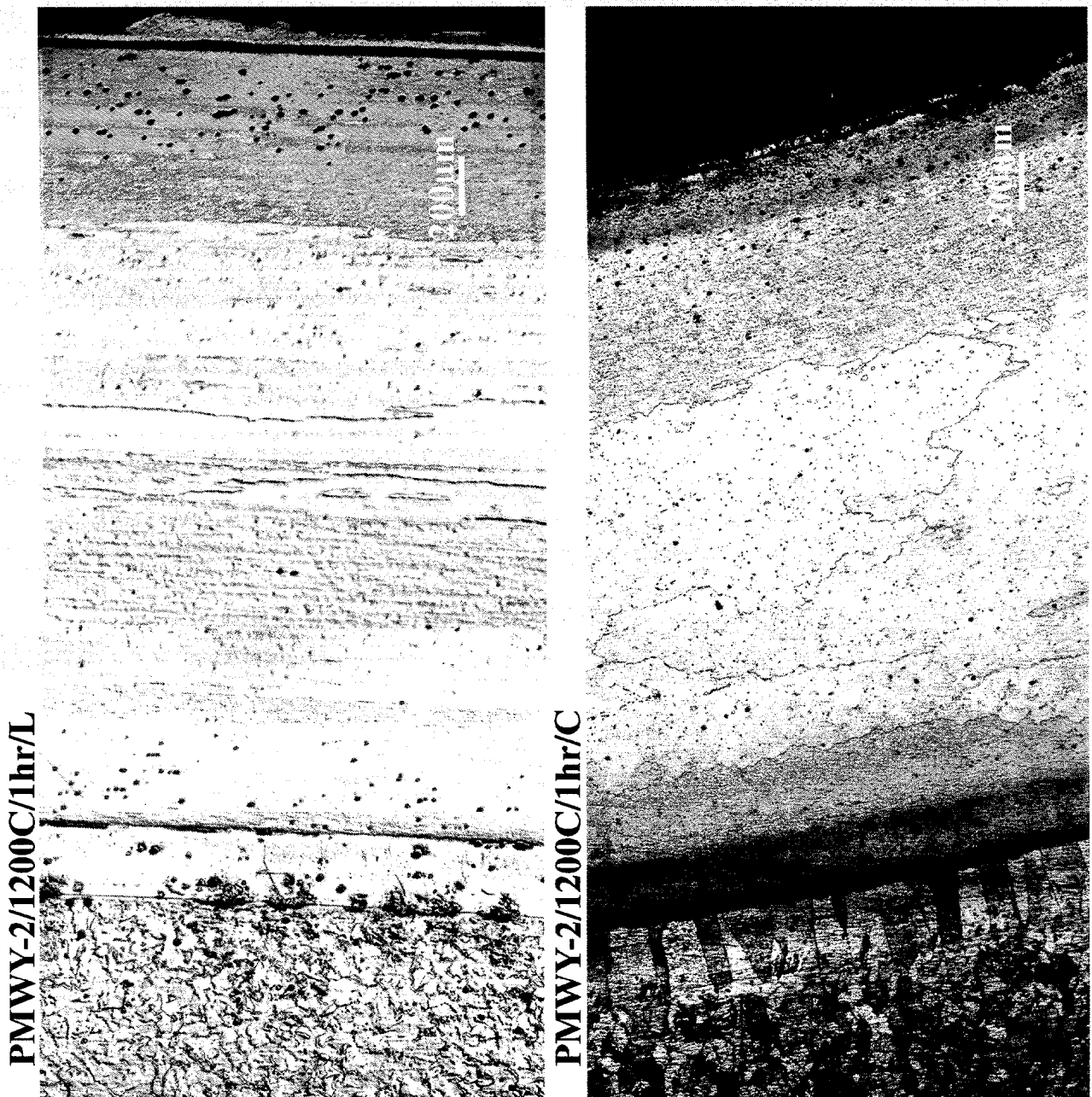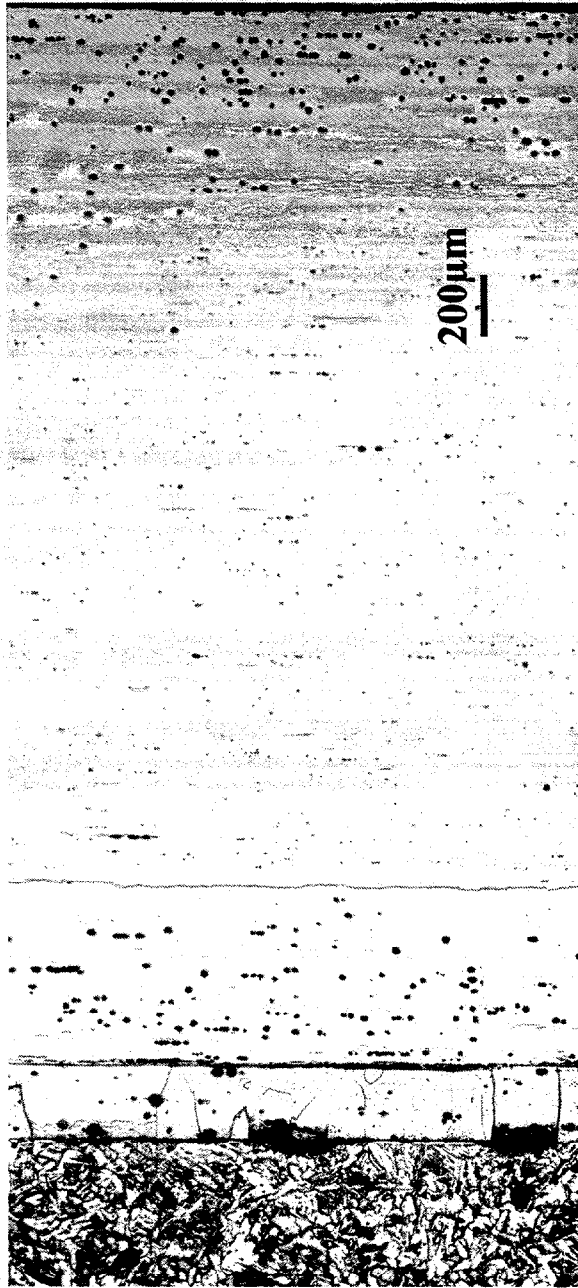Figure 16. Longitudinal and transverse views of the PMWY-1 tube heat-treated at 1200°/1hr.

17

Figure 17. Longitudinal and transverse views of the PMWY-2 tube heat-treated at 1200°/1hr.
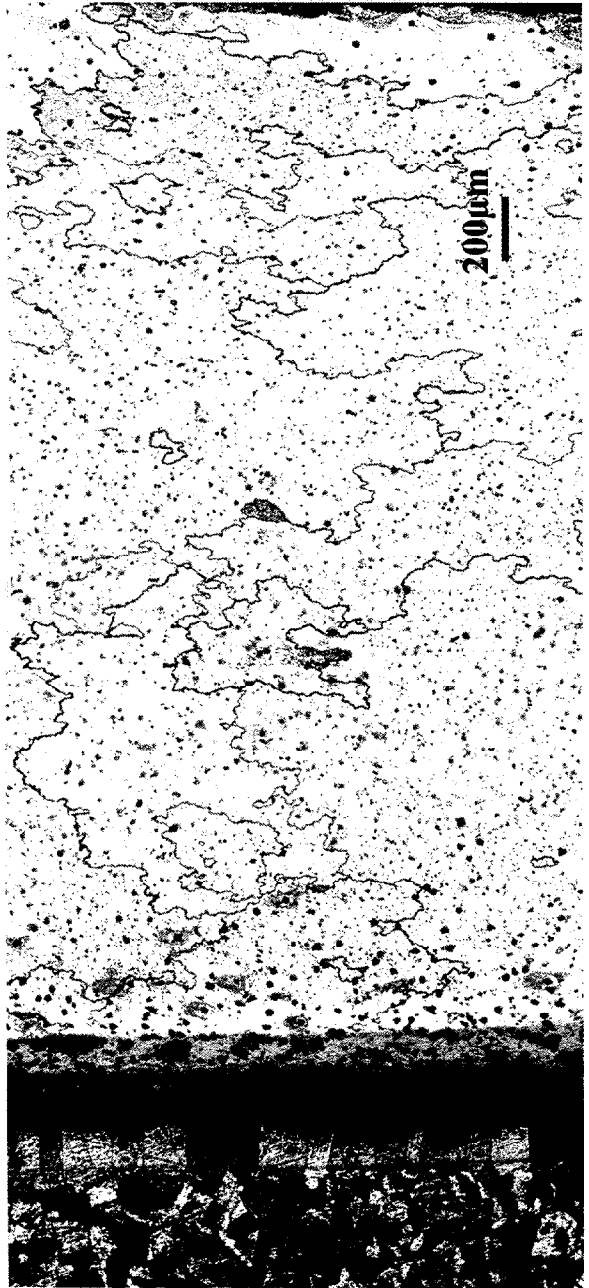
Figure 18. Longitudinal and transverse views of the PMWY-3 tube heat-treated at 1200°/1hr.

Progress: Iteration 4

Following the successful production of 1-3/8" OD extruded and recrystallized tubes in the preceding iteration, detailed microstructural and mechanical properties are examined in the current iteration.

A 10" long piece of each tube (PMWY-1, PMWY-2 and PMWY-3) was cut from the bulk stock and specifically heat-treated in a muffle furnace at 1200°C for 1-hr. Both TEM and mechanical property specimens were extracted from this tube. Thus, in the following sections, unless stated otherwise all samples are taken from these extruded tubes.

TEM Microstructures

Bright Field TEM micrographs of specimens extracted from the heat-treated tubes are shown in Figure 19. The 3mm discs were extracted from the wall thickness of the tubing such that foil normal and the extrusion axis are co-incident. With the TEM thin foil perforation expected near the center of the discs, the microstructures shown below are then representative of the center of the tube thickness. Both PMWY-1 and PMWY-2 tubes exhibit a fine-grained structure, Figure 19a,b, with a <110> fiber texture indicating incomplete recrystallization. However, PMWY-3, Figure 19c, exhibits a coarse grain structure with a <111> fiber orientation. The precipitate distribution in PMWY-3 is bi-modal with the coarser particles exhibiting a cell-type structure on the scale of 1 μm. This dimension is consistent with the as-extruded grain size and it is suggested that this particle distribution was originally present at the as-extruded grain boundaries.
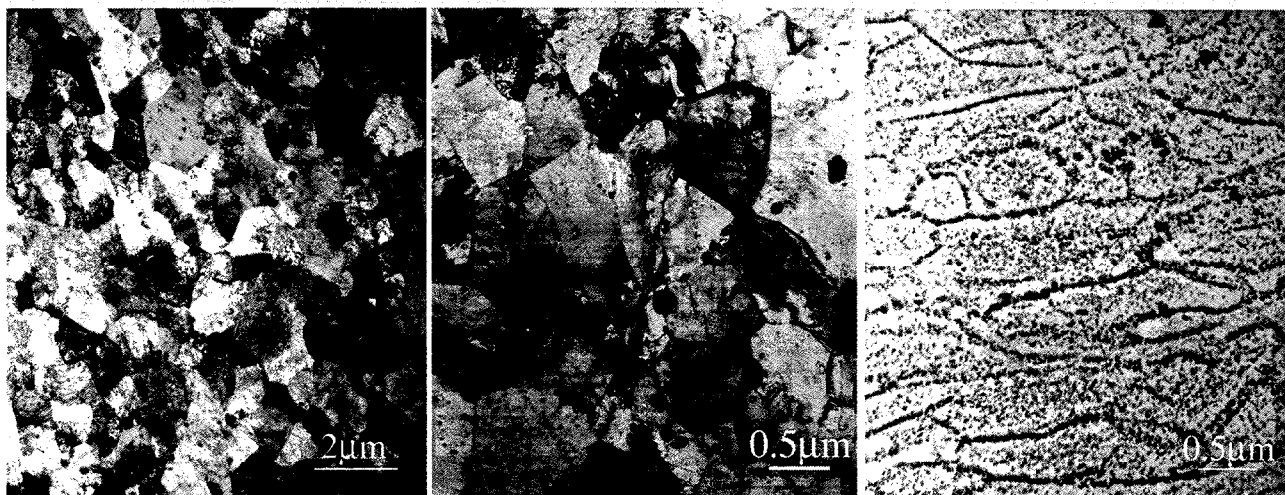
Figure 19. TEM micrographs of a) PMWY-1, b) PMWY-2 and c) PMWY-3 specimens extracted from the heat-treated tubes. The viewing direction is along the extrusion axis.

We note that PMWY-2 often shows large recrystallized regions or fine grains depending on where the thin foil for TEM studies is extracted. A magnified view of the PMWY-2 sample, Figure 20, reveals that the grains are effectively pinned by fine (Figure 20a) and coarse (Figure 20b) precipitate particles. As shown later the large particles are typically oxides and nitrides of aluminum and are most commonly encountered at the grain boundaries and vertices.
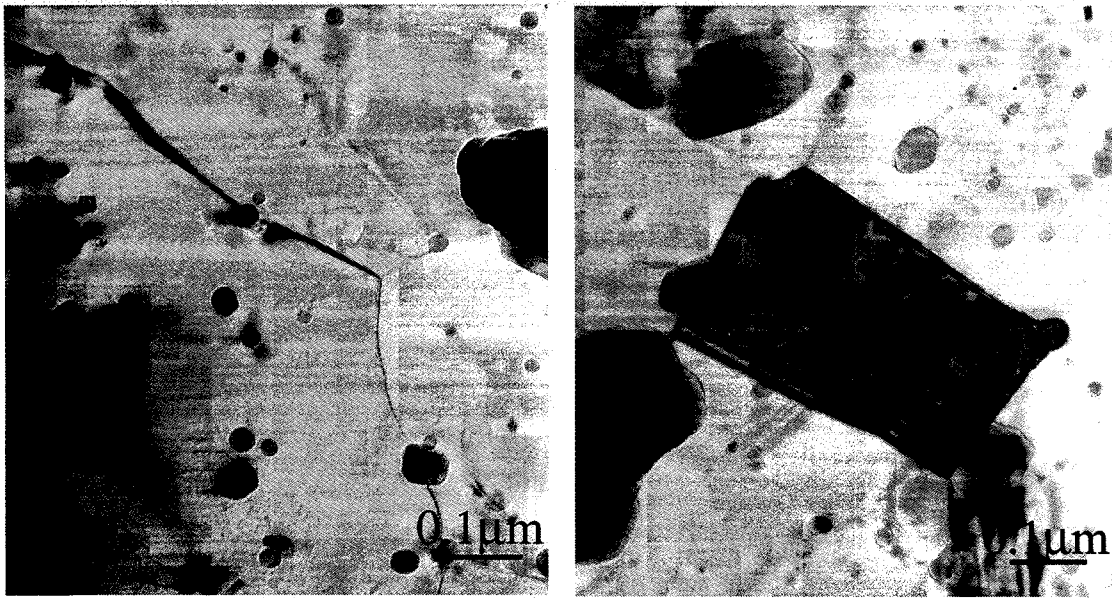
Figure 20. Magnified view of PMWY-2 tube cross-section indicating the pinning of grain boundaries by a) small yttrium oxide, and b) large (AlN or Al_2O_3) precipitate particles.

Precipitate Chemical Analyses

The precipitate chemistry was analyzed by EDS primarily for as-extruded and heat-treated OMWY-2 tubes. The bulk of the large precipitates (0.1-0.2μm as shown in Figure 20b) were identified as oxides, nitrides of aluminum as shown in Figure 21a,b and Table 5,6. Despite the presence of a healthy C impurity level (see Table 1) no large carbide precipitates were observed.

Figure 21. EDS Spectra of a) aluminum nitride, and b) aluminum oxide in PMWY-2 foils.

Table 5: Chemical Analysis of Aluminum Nitride precipitate (Figure 21a)

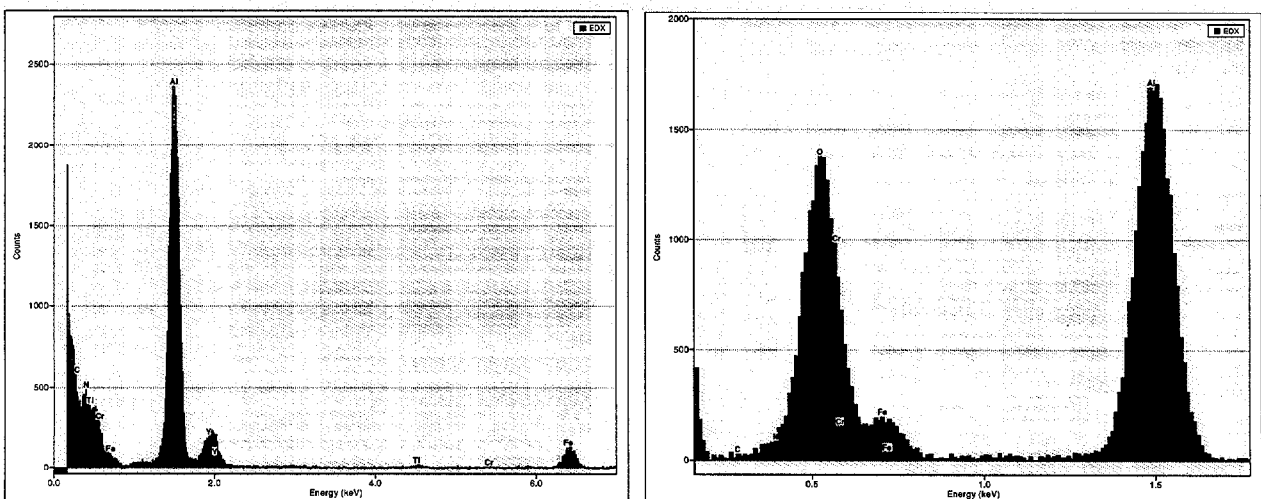| Edge	Intensity	k-factor	Weight %	Atomic %
N Kα	3792	3.920	30.62	48.91
Al Kα	26617	1.039	56.98	47.26
Ti Kα	54	1.308	0.15	0.07
Cr Kα	34	1.385	0.10	0.04
Fe Kα	1441	1.488	4.42	1.77
Y Kα	1026	3.659	7.73	1.95

Table 6: Chemical Analysis of Aluminum Oxide precipitate (Figure 21b)

Edge	Intensity	k-factor	Weight %	Atomic %
O Kα	13833	1.950	50.96	67.13
Al Kα	18399	1.039	36.13	28.22
Cr Kα	155	1.385	0.40	0.16
Fe Kα	3869	1.488	10.87	4.10
Y Kα	236	3.659	1.63	0.39

The Yttrium Oxide particles are in general much finer (see Figure 20a) and are often present as complex oxides of aluminum, iron and yttrium. An example spectrum is shown in Figure 22 where the particle is analyzed in Table 7 as yttrium-aluminum-oxide (also known as garnet).
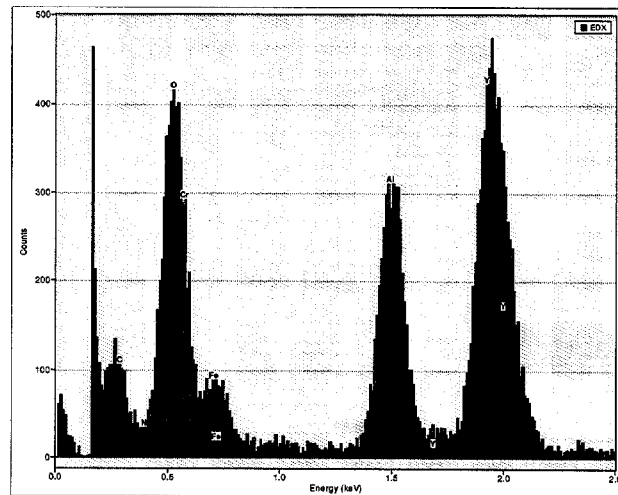
Figure 22. Figure 21. EDS Spectra of yttrium-aluminum-oxide (YAG) in PMWY-2 foils.

Table 7: Chemical Analysis of Yttrium-Aluminum Oxide precipitate (Figure 20a)

Edge	Intensity	k-factor	Weight %	Atomic %
O Kα	4289	1.950	34.01	64.54
Al Kα	3284	1.039	13.88	15.62
Cr Kα	24	1.385	0.14	0.08
Fe Kα	1647	1.488	9.97	5.42
Y Lα	4082	2.530	42.01	14.34

Progress: Iteration 5

High Temperature Mechanical Response

High temperature tensile properties were examined for ASTM E-8 miniature specimens spark machined from the 1/8" shell thickness of the 1-3/8" O.D. extruded tube. Tensile test were performed at temperature at a constant strain rate of 3×10^{-3} sec^{-1}.

Figure 23 shows the strength and ductility response for recrystallized PMWY-2 tube stock tested over the room temperature to 1100°C range. Figure 23a indicates that the material exhibits a strength plateau up to 400°C with large drops experienced in the 400-800°C range. In the anticipated service temperature range of 900-1100°C the material response is elastic-fully plastic, with the YS ranging from 8-14Ksi. Figure 23b indicates that both ductility and reduction in area (RA) go through a maxima at about 800°C. The change in RA beyond 800°C is particularly noteworthy. As shown later this is indicative of a change in active deformation mechanism.
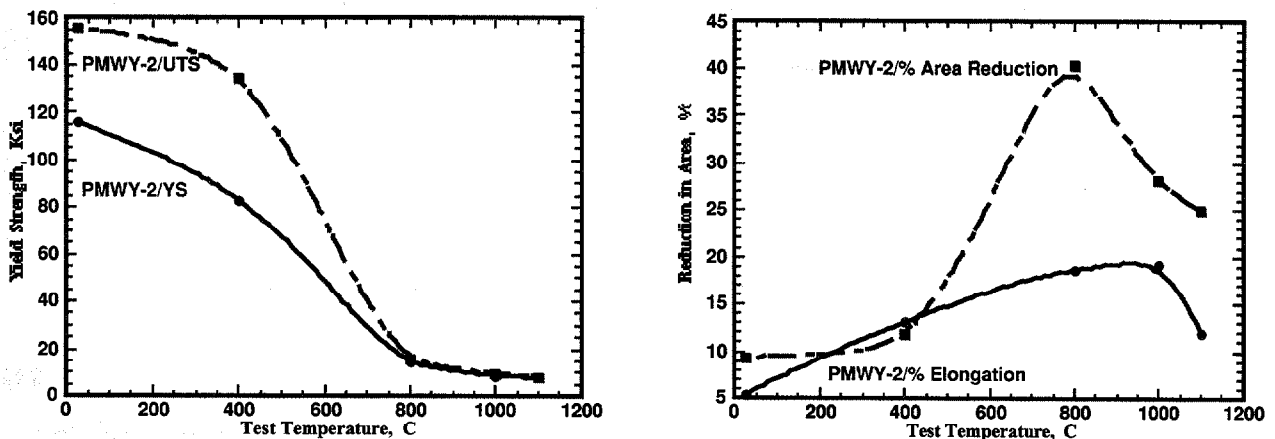
Figure 23. a) Strength and b) ductility response of extruded and recrystallized PMWY-2 stock.

Figure 24 shows the failure microstructures for PMWY-2 tensile coupons (ASTM E-8 specimens with ½" gage length) tested over a range of temperatures at a strain rate of 3×10^{-3} sec^{-1}. The material exhibits brittle fracture at the lower temperatures and ductile fibrous fracture at 1000°C and above yielding a brittle to ductile transition temperature (DBTT) of about 800°C. The fracture mode transition at about 800°C reflects a change in deformation mechanism from a dislocation-dominated glide to a diffusion assisted deformation mechanism. For example, the complete necking of figure 24c indicates dominant dislocation glide mechanisms, and the gradual drop in %RA (Figure 23b) beyond this temperature suggests subtle shifts in mechanisms operative at this particular strain rate of testing. The maximum % reduction in area at 800°C (Figure 23b) is entirely consistent with the chisel shaped fracture evidence of Figure 24c, where the specimen has gage thickness is essentially reduced to a line. Fracture evidence for the 1100°C tensile test reveal similar, but finer, features as shown in Figure 24d. For Brevity only the failure fractures of PMWY-2 are illustrated here. Fracture surfaces in PMWY-2 and PMWY-3 exhibit essentially similar behavior, with minor differences in strength and ductility levels.
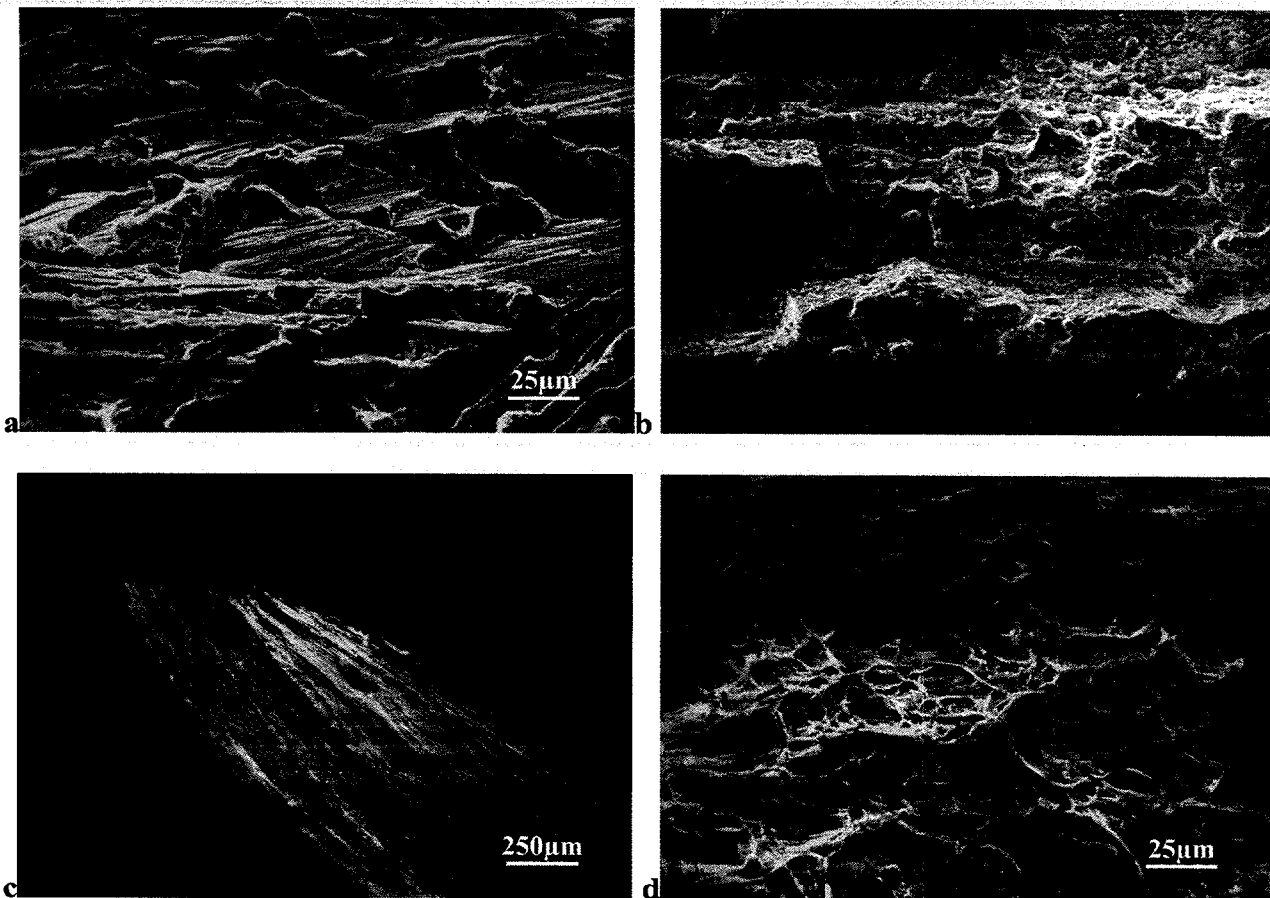
Figure 24. Tensile failures in PMWY-2 specimens tested at a) Room-Temp, b) 400°C, c) 800°C, and d) 1000°C. Note complete necking for the 800°C test with a corresponding maximum reduction in area.

With the DBTT established in the previous iteration, the anticipated service temperature identified as greater than 800°C and the constancy of the fracture mechanism beyond this temperature, further tests were limited to the 800-1000°C range for all the three tubes. Tables 8,9 list the complete matrix of tests conducted in the longitudinal orientation and transverse orientations, respectively. In each table, the samples are identified as PMWY-1, PMWY-2 and PMWY-3 and the second identifier is the batch order in which the tests were conducted. The composite behavior of all specimens is for the longitudinal and transverse orientations is given in figures 25a,b. Using tensile strength as a ranking measure for the peak test temperature of 1000°C we note that for longitudinal testing PMWY-3 exhibits the best combination of yield and ultimate tensile strength. Selected samples of PMWY-2 matched the mechanical response of PMWY-3 while PMWY-1 exhibited the poorest response. Because of the significant scatter in mechanical response, it was surmised that possible furnace temperature gradients might cause point-to-point variations in microstructure. As a result, machined ASTM specimens (batch 4) of PMWY-1 and PMWY-2 were heat-treated again at 1200°C-1hr and retested. We note that PMWY-1 exhibits a modest improvement in strength at the higher 1000°C test temperature. Further heat-treatments of such samples are continuing to explore additional improvements in high temperature response.

Table 8. High Temperature Longitudinal Mechanical Properties for the Extruded Tubes

Sample	Heat Treatment	Test Temp	YS, Ksi	UTS, Ksi	Elongation
PMWY-1, 1st*	1200C/1hr, Air	800.00	14.900	18.700	25.500
PMWY-1, 2nd*	1200C/1hr, Air	800.00	15.900	18.100	30.700
PMWY-1, 3rd*	1200C/1hr, Air	800.00	18.400	18.600	23.700
PMWY-1, 4th	1200C/1hr, Air	800.00	18.900	20.100	28.500
PMWY-1, 1st*	1200C/1hr, Air	900.00	10.900	11.700	30.000
PMWY-1, 2nd*	1200C/1hr, Air	900.00	15.100	15.400	22.700
PMWY-1, 3rd*	1200C/1hr, Air	900.00	13.800	14.100	43.700
PMWY-1, 4th	1200C/1hr, Air	900.00	13.400	13.800	30.500
PMWY-1, 1st*	1200C/1hr, Air	1000.0	7.9000	9.1000	45.900
PMWY-1, 2nd*	1200C/1hr, Air	1000.0	8.8000	9.3000	25.700
PMWY-1, 3rd*	1200C/1hr, Air	1000.0	9.4000	9.7000	17.600
PMWY-1, 4th	1200C/1hr, Air	1000.0	9.9000	10.400	31.000
PMWY-2, 1st*	1200C/1hr, Air	800.00	15.900	18.700	27.000
PMWY-2, 2nd*	1200C/1hr, Air	800.00	18.200	18.800	37.000
PMWY-2, 3rd*	1200C/1hr, Air	800.00	18.200	18.200	19.800
PMWY-2, 4th	1200C/1hr, Air	800.00	20.800	20.900	19.000
PMWY-2, 1st*	1200C/1hr, Air	900.00	11.400	12.100	36.000
PMWY-2, 2nd*	1200C/1hr, Air	900.00	12.400	13.100	22.500
PMWY-2, 3rd*	1200C/1hr, Air	900.00	13.800	14.700	10.800
PMWY-2, 4th	1200C/1hr, Air	900.00	13.000	13.700	17.800
PMWY-2, 1st*	1200C/1hr, Air	1000.0	11.400	11.600	13.700
PMWY-2, 2nd*	1200C/1hr, Air	1000.0	12.400	13.600	11.500
PMWY-2, 3rd*	1200C/1hr, Air	1000.0	12.100	12.200	9.2000
PMWY-2, 4th	1200C/1hr, Air	1000.0	11.400	11.900	21.200
PMWY-3, 1st	1200C/1hr, Air	800.00	19.600	20.900	10.000
PMWY-3, 3rd	1200C/1hr, Air	800.00	19.300	20.900	10.200
PMWY-3, 1st	1200C/1hr, Air	900.00	12.500	14.400	6.0000
PMWY-3, 3rd	1200C/1hr, Air	900.00	16.600	16.700	7.7000
PMWY-3, 1st	1200C/1hr, Air	1000.0	9.4000	12.800	10.200
PMWY-3, 3rd	1200C/1hr, Air	1000.0	12.200	13.200	6.1000

*Samples extracted from heat-treated tubes. For the 4th batch, the ASTM samples were reheated at 1200°C-1hr prior to testing as furnace gradients are assumed to cause point to point variations in the recrystallized microstructure. Modest improvement is noted in PMWY-1 as a result of this re-heat treatment.

Table 9. High Temperature Transverse Mechanical Properties for the Extruded Tubes

Sample	Heat Treatment	Test Temp.	YS, Ksi	UTS, Ksi
PMWY-1, 3rd	1200C/1hr, Air	800.00	15.800	18.600
PMWY-1, 4th	1200C/1hr, Air	800.00	17.800	20.100
PMWY-1, 3rd	1200C/1hr, Air	900.00	10.000	11.100
PMWY-1, 4th	1200C/1hr, Air	900.00	10.100	11.000
PMWY-1, 3rd	1200C/1hr, Air	1000.0	11.300	11.700
PMWY-1, 4th	1200C/1hr, Air	1000.0	8.0000	8.4000
PMWY-2, 3rd	1200C/1hr, Air	800.00	16.200	16.300
PMWY-2, 4th	1200C/1hr, Air	800.00	16.600	17.800
PMWY-2, 3rd	1200C/1hr, Air	900.00	10.600	11.100
PMWY-2, 4th	1200C/1hr, Air	900.00	10.400	11.200
PMWY-2, 3rd	1200C/1hr, Air	1000.0	11.800	12.100
PMWY-2, 4th	1200C/1hr, Air	1000.0	4.1000*	4.3000*
PMWY-3, 3rd	1200C/1hr, Air	800.00	18.600	19.100
PMWY-3, 3rd	1200C/1hr, Air	900.00	12.400	12.800
PMWY-3, 3rd	1200C/1hr, Air	1000.0	11.200	11.200

Samples extracted by multiple forging split tube sections at 900°C. Multiple forging steps were required with the specimen given a 15minute soaking treatment at 900°C. All samples given a final anneal of 1/2hr at 900°C.

The tabulated test data provided in Tables 8 and 9 is graphically illustrated in Figures 25a,b for the longitudinal and transverse orientations, respectively. Note that the fully recrystallized microstructure of PMWY-3 specimens (see Figure 19c) exhibits the best performance for both the longitudinal and the transverse oriented specimens. There are subtle variations in the longitudinal and transverse strength response for the respective powder batches. For example all the three powder batches show some work hardening in the longitudinal orientation absent in the transverse orientations. For PMWY-1 and PMWY-3 the transverse strength closely follows the longitudinal strength (albeit a little inferior) but a 50% drop is observed for the PMWY-2 samples. This is likely attributed to the point-to-point variations in the recrystallized microstructure that may contain isolated un-recrystallized regions.

The transverse orientation specimens were initially produced by hand forging heat-treated tubes into flat sections. Multiple forging steps were required with intermittent 10 min anneals at 900°C, followed by a final anneal of ½ hour. This procedure has been modified to a single step forging of as-extruded tubes followed by recrystallization. These test are currently in progress.

Looking forward to the next section (Progress: Iteration 5) we note that the creep response is particularly affected by the underlying grain structure. In an effort to improve overall grain growth in PMWY-1 and PMWY-2, ASTM E-8 tensile specimens were given additional thermal treatments (1200°C-1hr) and re-tested (results identified as batch 4 tests in Table 9). With the exception of PMWY-1 tested at 1000°C, the results are inconclusive. Nonetheless, looking to forward to the next section marginal improvements in creep response are being recorded.

Mechanical Response of the Powder Batches

a)

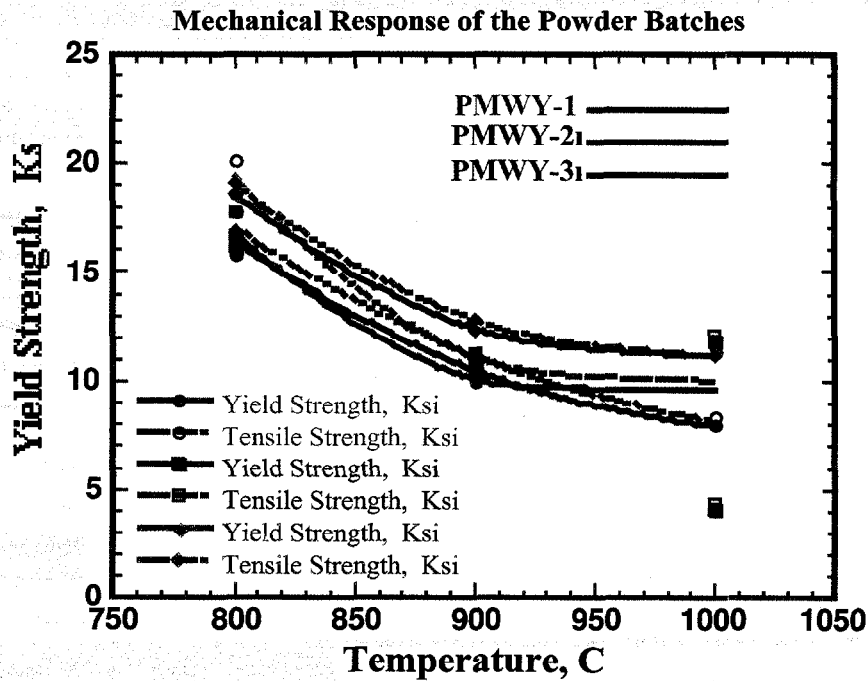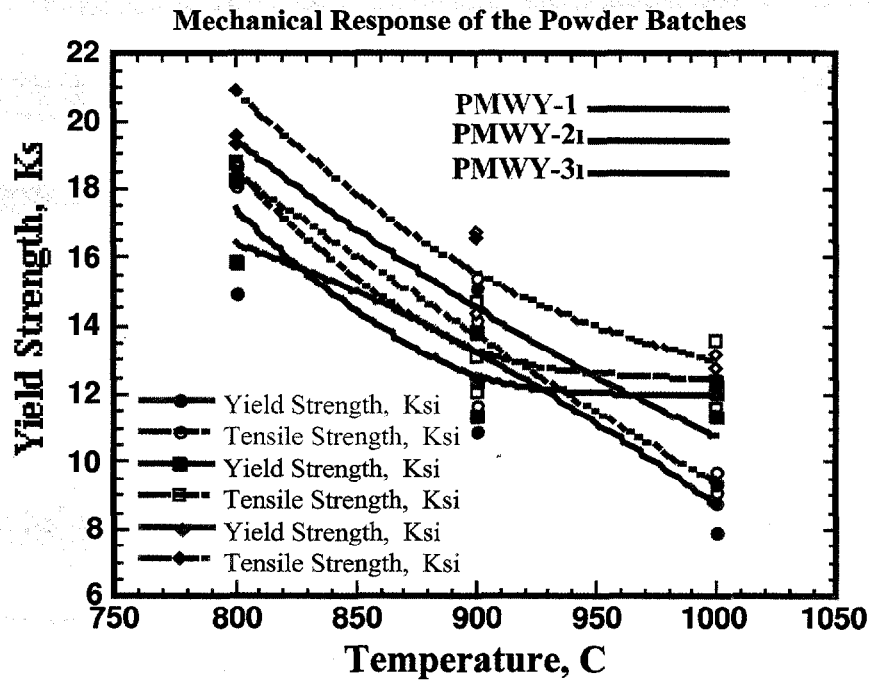**Mechanical Response of the Powder Batches**

b)

Figure 25. High temperature mechanical response for the a) Longitudinal and b) Transverse orientations. The fully recrystallized microstructure of PMWY-3 (See Figures 18, 19) offers the best response over the entire test-temperature range in either orientation.

Progress: Iteration 6

High Temperature Creep Response

An evaluation of high temperature creep response was not initially tasked in this program. However, all current program development is intended to improve creep response. Fortunately a large data-base for ODS material creep-response is being assembled at ORNL by Dr I. G. Wright and Claudette McKamey. Thus, efforts are in process to measure the longitudinal and transverse creep-response of processed tubes in collaboration with ORNL. Limited creep tests results are presented in Table 10 , 11 for the longitudinal and transverse orientation respectively.

Table 10. Longitudinal Stress-Rupture tests at 1000°C; constant load test

Sample	Loading	Elongation	Life (Hrs)
PMWY-1	Constant, 3 Ksi	2.4%	147.3
PMWY-1	Constant, 3 Ksi	7.3%	45.4
PMWY-1	Incremental, 2-4 Ksi	3.7%	248.0
PMWY-1	Constant, 5 Ksi	-	1.9^
PMWY-1**	Constant, 5 Ksi	-	46
PMWY-2	Incremental, 2-4 Ksi	3.0%	328.3*
PMWY-2	Constant, 5 Ksi	-	63.7*
PMWY-2	Constant, 6 Ksi	2.6%	4.3
PMWY-2	Incremental, 3-7 Ksi	-	636.0*
PMWY-2	Constant, 7 Ksi	-	55.4^
PMWY-3	Incremental, 5-10 Ksi	-	777
PMWY-3	Constant, 9 Ksi	-	636

Specimens heat-treated in air at 1200°C-1hr; constant load test, *specimens failed outside the gage length at the pinhole, **test repeated after re-annealing the ASTM-E8 specimen at 1200°C –1hr in air, ^test at UCSD.

Table 11. Transverse Stress-Rupture tests at 1000°C; constant load test

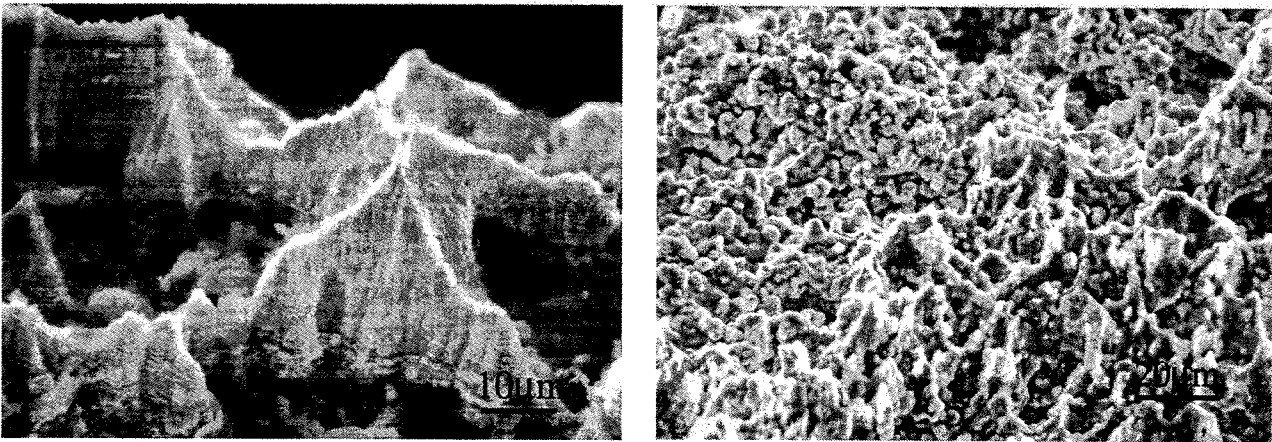| Sample	Loading	Elongation	Life (Hrs)
PMWY-2T	Constant, 5 ksi	-	0.2
PMWY-2T	Constant, 5 ksi	-	14.7
PMWY-3T	Constant, 5 ksi	-	0.3
PMWY-3T	Constant, 5 ksi	-	2.0

Figure 26. Stress rupture fractures in a) PMWY-1 incrementally loaded at 2-4 Ksi at 1000°C, life=248hrs, and b) PMWY-2 loaded at 6 Ksi at 1000°C, life =4.3 hours. Differences in failure substructure are related to the underlying grain structure developed during heat-treatments.

With reference to the Table 10 (longitudinal test results), we note that PMWY-3 exhibits the best performance till date followed by PMWY-2 with PMWY- exhibits the poorest performance. Such differences are directly related to the underlying grain structure developed in these alloy tubes at the constant heat-treatment temperature of 1200°C-1hr as indicated in the optical micrographs of Figures 16-18 and the transmission electron micrographs of Figure 19. Thus PMWY-1 with the bulk of the un-recrystallized regions across the tube wall exhibits poor creep response. The scatter in PMWY-2 response derives from the exact location in the tube wall where the specimen is spark machined. Since PMWY-2 exhibits incomplete recrystallization, such local factors determine the fraction of fine grain constituent include in the ASTM E-8 specimen gage thickness. Figure 26 illustrates the striking difference in fractures for the fine and coarse-grained materials. Fine grained PMWY-1 exhibits high ductile lobes in crept specimens, Figure 26a, whereas no such features are observed in coarse-grained PMWY-2, Figure 26b, or in PMWY-3. Such fracture features therefore offer subtle clues to the underlying grain structure.

ASTM E-8 specimens of PMWY-1 and PMWY-2 were re-heat treated at 1200°C-1hr to promote grain coarsening. Initial test on a PMWY-1 specimen (labeled ** in Table 10) exhibits the best response recorded till date. Further tests are planned to explore this promising trend.

Creep Deformation Response Microstructures

Deformation substructures have been examined for high temperature tensile tests and creep tests particularly in fully recrystallized rods and tubes. Deformation microstructures observed in tensile tests are essentially glide dominated, with <111> dislocations gliding on {110} planes. However, the deformation sub-structure under creep conditions evolves with specific conditions of temperature and stress. Two specific cases are illustrated here.

i) Low Temperature-High Stress

Figure 27 shows deformation substructure in a region immediately below the fracture surface for a PMWY-2 rod specimen creep tested at 900°C at 7Ksi. At this temperature, the

deformation, at least close to the fracture region is comprised of glide dislocations confined to their respective slip planes. For a nominal stress-rupture testing axis of [$\bar{1}$11], as is the case for fully recrystallized specimens along the extrusion axis, the operating slip planes are found to be (110), Figure 27b, and (0$\bar{1}$1), Figure 26c, with Burgers vectors b=1$\bar{1}$1 and 111, respectively. Both slip planes and glide dislocations are visible in Figure 26a.

A single dislocation loop (in the center of the micrograph) exhibits cross-slip/climb behavior suggesting that some climb processes are operative even under what may be a fast fracture process. This combination of glide and climb processes is consistent with the DBTT and the prior observation in the fracture morphology changes in tests conducted above 800°C.

Figure 27. Deformation substructure in creep tested (900°C-7Ksi) PMWY-2 rod specimens.

ii) High Temperature-Low Stress

Figure 27 shows deformation substructure in a region immediately below the fracture surface for a PMWY-2 rod specimen creep tested at 1000°C at 5Ksi. The deformation substructure is no longer dominated by glide – and no dominant slip plane activity is observed. The <111> type dislocations are pinned by fine Y_2O_3 (or $Y_2O_3.Al_2O_2$) precipitates, and in the process of climb. The dislocations exhibit a characteristic g.b=0 or g.bxu=0 type of invisibility contrast for g=022, Figure 27c, and g=202, Figure 27d, yielding a Burgers vector b=1$\bar{1}$1. Furthermore, the dislocation edge segments cannot be reconciled to likely slip planes. The deformation at this stage is therefore dominated by diffusion controlled climb events.

Two features of the microstructure are of additional interest. In the bi-modal precipitate distribution of Figure 29a one set of precipitates (at the prior grain/particle boundaries) shows significant strain contrast under 2-beam imaging conditions. This particular precipitate appears to trap some dislocations presumably as an energetic process of lowering its strain energy. Figure 29b shows that fine particles (typically 10-20nm) are particularly suited for dislocation pinning in the climb regime. These particles then are the yttrium oxides (or $Y_2O_3.Al_2O_2$) and not the impurity oxides or nitrides of aluminum (as identified by quantitative EDS).
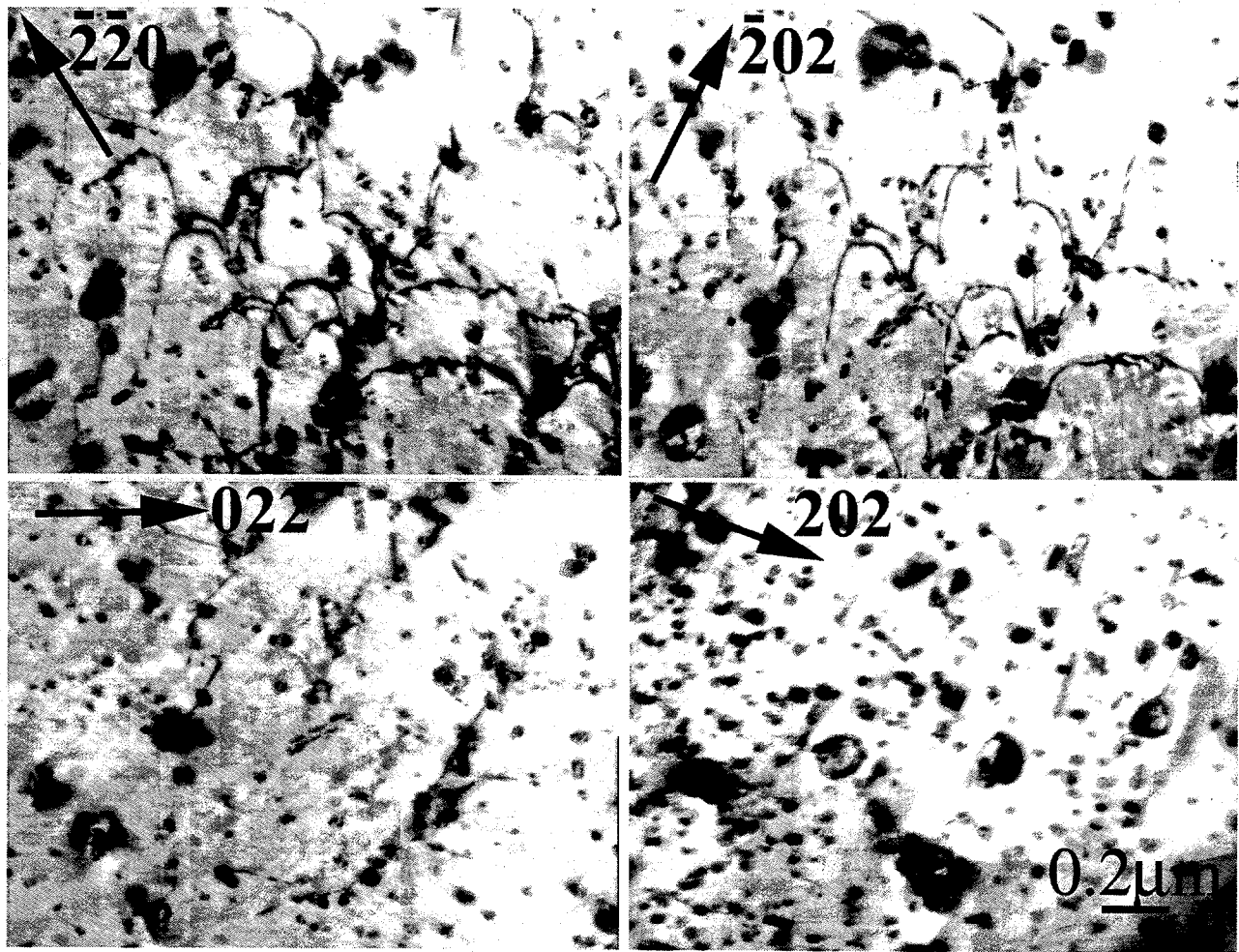
Figure 28. Deformation substructure in creep tested (1000°C-5Ksi) PMWY-2 rod specimens.
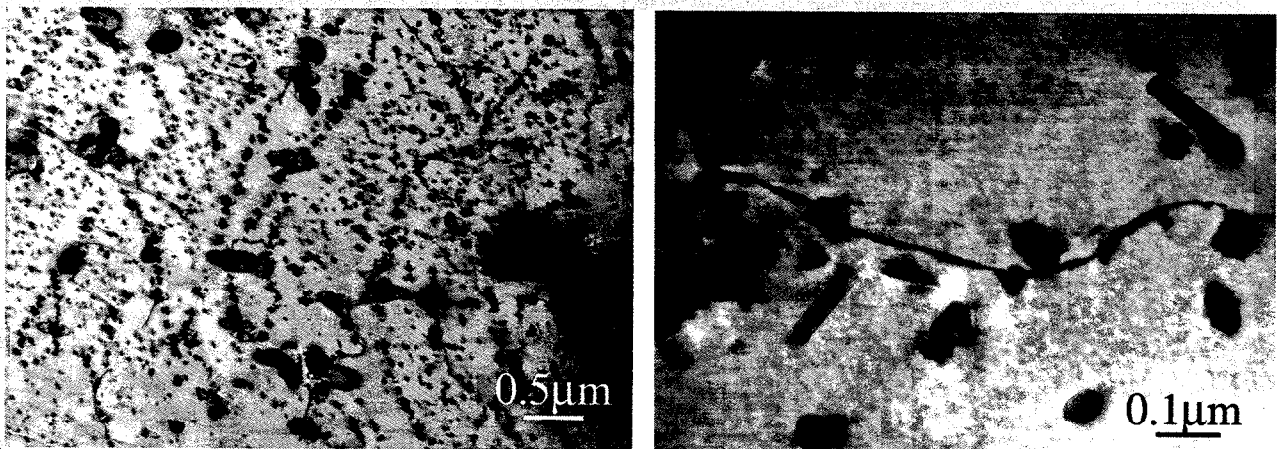

Figure 29. Deformation substructures in crept PMWY-2 specimens. A) Tested at 1000°C at 5Ksi. Note strain contrast around selected precipitates that trap dislocations. b) Tested at 1050°C at 3-6Ksi where fine Y_2O_3 precipitates offer the best dislocation pinning response.

Summary and Conclusions

The oxide dispersion strengthened (ODS) Fe_3Al-based alloy powders (PMWY-1, PMWY-2, PMWY-3) were successfully consolidated into solid rods and tubes by the single step hot extrusion methodologies. The creep performance ODS-Fe_3Al materials has been initially studied in Longitudinal and to a limited extent in the Transverse orientations, and deemed acceptable within the prescribed performance envelope. It is interesting to note that grain growth kinetics are affected by interstitial impurity content, which limit the extent of recrystallized regions observed in the tube wall. Consequently, the microstructures exhibiting the best creep response (i.e., PMWY-3) are ones that undergo complete recrystallization. Such creep performance will continue to be evaluated specifically for the tube specimens in the next phase of the research program. The following conclusions are possible based on our studies till date:

1. The ODS-Fe_3Al rods and tubes can be fully consolidated at 1000°C and at extrusion ratios of about 16:1, while exhibiting reasonable post-extrusion recrystallization kinetics.

2. Recrystallization is initiated in all powder batches heat-treated at 1200°C-1hr with recrystallized grain sizes of the order of 200-5000μm. However the growth kinetics are affected by the overall interstitial impurity content, such only partial wall section of the tube undergoes large-scale grain growth.

3. Secondary grain growth kinetics exhibit an direct relationship with the total interstitial impurity content of the milled powder batches, with the purest batch PMWY-3 exhibiting the most favorable grain growth.

4. Creep response if the respective powder batches is proportional to the underlying grain structure produced via heat-treatments. Thus powder batch PMWY-3 with the complete recrystallized section offers the best creep response.

5. Powder batch milling appears to be the single most pervasive processing component dominates microstructural and material response. It is suggested that coarse nitrides and oxides of aluminum (formed during milling) while inhibiting recrystallization grain growth (as observed in PMWY-2 and PMWY-3) are ineffective in dislocation pinning in the climb regime. Effective pinning is only provided by the fine Y_2O_3 and $Y_2O_3.Al_2O_3$ precipitates.

6. Preliminary efforts to enhance the growth kinetics in PMWY-1 and PMWY-2 primarily by prolonging the hold time at 1200°C improve the ensuing creep response incrementally.

Acknowledgements

References

1. V.K. Sikka, S. Vishwanathan, C.G. McKamey, 1993, <u>Structural Intermetallics</u>, (TMS) 483

2. P.G. Sanders, V.K. Sikka, C.R. Howell, R.H. Baldwin, 1991, <u>Scripta Met.</u>, **25**, 2365.

3. I.G. Wright, B.A. Pint, E.K. Ohriner and P.F. Tortorelli, 1996, *Proc. 11th Ann. Conf. on Fossil Energy Materials*, ORNL Report ORNL/FMP-96/1, CONF-9605167, p. 359

4. V.K. Sikka, I.G. Wright and B.K. Kad, *Proc. 12th Ann. Conf. Fossil Energy Materials*, Knoxville, TN, May 1998.

5. B.K. Kad, S.E. Schoenfeld, R.J. Asaro, C.G. McKamey, V.K. Sikka, 1997, <u>Acta Metall.</u>, **45**, No.4, p. 1333.

6. B.K. Kad, V.K. Sikka and I.G. Wright, *13th Ann. Conf. Fossil Energy Materials*, Knoxville, TN, May 1999

7. B.K. Kad, R.N. Wright, I.G. Wright and V.K. Sikka, *14th Ann. Conf. Fossil Energy Materials*, Knoxville TN, May 2000.